

**Metal in polymer: hybridization enables new functions**

Journal:	<i>Journal of Materials Chemistry C</i>
Manuscript ID	TC-REV-08-2020-003810.R1
Article Type:	Review Article
Date Submitted by the Author:	01-Oct-2020
Complete List of Authors:	Wei, Zichao; University of Connecticut, Department of Chemistry Duan, Hanyi; University of Connecticut, Department of Chemistry Weng, Gengsheng; Ningbo University, He, Jie; University of Connecticut, Department of Chemistry

ARTICLE

Metals in polymers: hybridization enables new functions

Zichao Wei,^a Hanyi Duan,^b Gengsheng Weng,^{*c} Jie He^{*, a,b}Received 00th January 20xx,
Accepted 00th January 20xx

DOI: 10.1039/x0xx00000x

Adding metals in synthetic polymers is of broad interest to design multifunctional materials, particularly harnessing unique properties and functionalities not found in pure organic polymers. Other than simple emergence of the two, such hybridization often enables synergies to amplify the existing properties and/or create new properties not existing in either component. In this review, we highlight recent examples of metal/polymer hybrids based on either well-defined or ill-defined metal-ligand (M-L) coordination to design multifunctional materials. This review describes how the hybridization of metal ions and polymers complements each other synergistically in terms of their optical, mechanical and catalytic functionalities. Synthetic polymers once bound to metals enable the stimuli-responsive properties of metals and control over the luminescence of metals in response to the change of environment. As the second coordination sphere, synthetic polymers also enhance the reactivity of metal sites as a means to design bioinspired artificial enzymes. Additionally, the impact of the M-L coordination on the dynamic properties of polymers is summarized in the context of self-healable and tough materials built on the reversible network of interchangeable M-L coordination.

1. Introduction

Traditionally design of functional polymers relies on their chemical identity. Modifying polymers with specific chemical moieties endows them with the desired functionality. Taking the phase transition as an example, water-soluble polyacrylamide becomes thermoresponsive when simply replacing one H atom of the amide group by an isopropyl moiety, known as poly(*N*-isopropylacrylamide) (PNIPAM).¹ PNIPAM shows a lower critical solution temperature (LCST, around 32 °C), reversible phase transition in water. Not surprising, the LCST of poly(*N*-alkyl substituted acrylamide) is highly tunable by varying such chemical identity, *e.g.*, the alkyl groups or copolymerization with other monomers, as reported previously.^{2, 3} In those systems, single functionality can be added-in or varied through synthetic tools similar to that of thermoresponsiveness. Those materials with single functionality, however, unlikely meet the rising demands of mankind to design more efficient and sophisticated devices. Design of new materials integrated with different functions is of essential importance in response to such demands. Yet, there are profound challenges to design those multifunctional materials in terms of, i) solving the compatibility of various functions;⁴ and ii) evolving new functions not existing in organic polymers. For example, common

organic polymers that usually do not have single or unpaired electrons are not useful as a contrast agent in magnetic resonance imaging (MRI). One way to bring new functionalities to polymers is hybridization that has been of long practice in materials chemistry and engineering. An obvious case is to solve the thermal and electric conductivity of organic polymers through hybridization with carbon and metallic nanomaterials.

Metals broadly defined as metal ions, clusters and nanoparticles, have many unique properties and thus corresponded functionalities, *e.g.*, luminescence,⁵ magnetism,⁶ plasmon⁷ and catalysis.⁸ When bound or simply mixed metals with organic polymers, those properties can be added up to the resultant hybrids. Gadolinium (Gd³⁺) containing polymers as an example have strong relaxivity and low toxicity for MRI examination.⁹ Hybridization of those metal species with organic polymers not only simply offers merged properties of the two different components but also enables new synergies, *i.e.*, amplifying the existing functionalities or creating ensemble functionalities not existing in the two components. Those, again, have been of long practice in design of metal/polymer hybrids. Binding late transition metals with organic or polymeric chromophores can populate the triplet states that are of great interest in electroluminescent materials for light-emitting diodes and photovoltaics.¹⁰ Noble metal nanoparticles assembled by polymer ligands show the strong coupling of the plasmonic field, leading to new resonance peaks that cannot be found in either polymers or individual nanoparticles.¹¹⁻¹³ Such collective properties enable the new functionalities of those hybrids in colorimetric sensing,¹⁴ photocatalysis¹⁵ and enhanced Raman scattering.¹⁶ Coordinating catalytic inactive or less active metal cations with synthetic polymers can significantly improve their reactivity.¹⁷ As such, the presence of metal in organic polymers shows great potentials to drive the development of multifunctional materials.

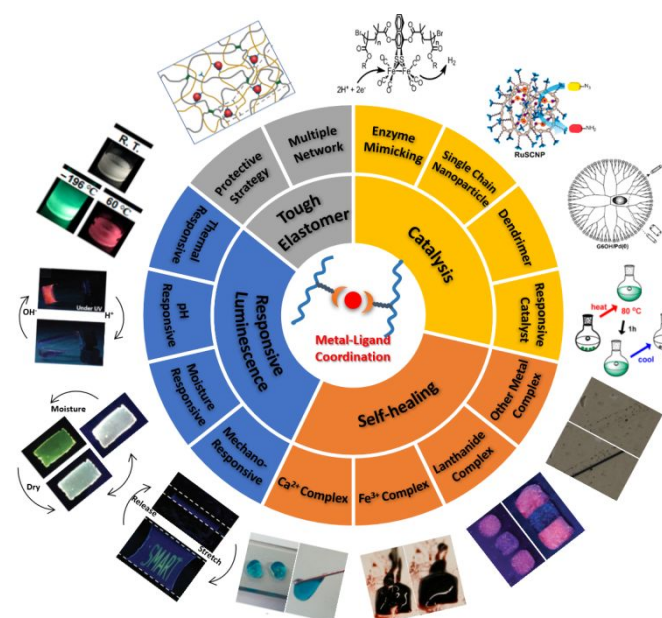
^a Department of Chemistry, Institute of Materials Science, University of Connecticut, Storrs, Connecticut 06269, United States; Email: jie.he@uconn.edu (JH)

^b Polymer Program, Institute of Materials Science, University of Connecticut, Storrs, Connecticut 06269, United States.

^c State Key Laboratory Base of Novel Functional Materials and Preparation Science, Ningbo Key Laboratory of Specialty Polymers, School of Materials Science and Chemical Engineering, Ningbo University, Ningbo, 315211, China. Email: wenggengsheng@nbu.edu.cn (GW)

† Footnotes relating to the title and/or authors should appear here.

Given the interdisciplinary nature, one of the key challenges in those metal/polymer hybrids is to understand their structure-function correlations. As mentioned in the broad definition of metals, hybridization of metals and polymers crosses size ranges from molecular and macromolecular to nanometer scales. There are a large body of works on multifunctional materials of metal/polymer hybrids that are not covered in this review, due to the limited knowledge of authors. For example, nanoclusters of noble metals/polyoxometalates and various metal nanoparticles can bind with polymers as well to design new multifunctional materials. We refer the interested readers to some of the excellent reviews on those topics by Kumacheva,¹⁸ Liu,¹⁹ Nie²⁰ and Tao.²¹ We will narrow our topics down to organic polymers incorporated with metal ions through metal-ligand (M-L) coordination as backbones or side chains. The focus of the current review is to highlight a few examples on metal/polymer hybrids based on either well-defined or ill-defined M-L coordination structures as multifunctional materials. The emphasis will be given on how hybridization of metals and polymers complements each other synergistically to enable the functionalities of resultant materials; that is, the uniqueness of each component to control the outcome of hybridization.



Scheme 1. Schematic summary of representative application areas derived from the polymeric metal-ligand interaction. (1) Blue regimes, responsive luminescence metal/polymer hybrids. Figures reproduced from Ref. 22, copyright 2015 American Chemical Society;²² Ref. 23, copyright 2018 Wiley VCH;²³ Ref. 24 and 25, copyright 2019 Wiley VCH.^{24, 25} (2) Orange regime, self-healable metal/polymer hybrids, figures reproduced from Ref 26, copyright 2017 American Chemical Society;²⁶ Ref. 27;²⁷ Ref. 23, copyright 2018 Wiley VCH;²³ Ref. 28, copyright 2019 Elsevier B.V..²⁸ (3) Yellow regime, catalysis of metal/polymer hybrids. figures reproduced from Ref. 29, copyright 2015 American Chemical Society;²⁹ Ref. 30, copyright 2001 American Chemical Society;³⁰ Ref. 31, copyright 2020 American Chemical Society;³¹ Ref. 32, copyright 2019 Wiley VCH.³² (4) Grey regime, tough elastic metal/polymer hybrids, figure reproduced from Ref. 24, copyright 2019 Wiley VCH.²⁴

First of all, binding metals varies the dynamics of polymer chains. As a typical example, metal cations that coordinate with a few ligands at one time can interact with polymer intermolecularly to result in non-covalent cross-links. The network built on dynamic M-L interactions instantly exchanges, *i.e.*, dissociate and reform at the same time. With any mechanical rupture of those hybrids, such non-covalent network can restructure to repair the damage through the dynamic exchange of M-L complexes, known as self-healable materials (Scheme 1). The healing efficiency is dependent on the M-L binding strength, the coordination number of metal sites and even the counter ions of metals, as summarized in Section 3. The reversible M-L interactions also makes it possible to dissipate the mechanical energy upon deformation that largely improves the toughness of polymers. Using M-L coordination together with a strong network formed by covalent cross-linking, one can design tough elastic materials highly resistant to mechanical failure, as discussed in Section 4. On the other hand, polymers show a great impact on, or determine in some cases, the functionalities of metals (Scheme 1). We review some recent advances in stimuli-responsive luminescent metal/polymer hybrids with a particular emphasis on emissive lanthanides. We highlight two design mechanisms based on coordination disruption and coordination competition to switch ON/OFF the emission of lanthanides in Section 2. At the end, we discuss the synergies of synthetic polymers to the catalytic activity of metal ions. The role of synthetic polymers, particularly the positive effect to the reactivity of metal sites, is spotlighted as a means to design bioinspired artificial enzymes. We would like to point out that many other functionalities of coordination polymers, such as electroluminescence,³³ antifouling,³⁴ and magnetism,⁶ have not been included in the current review.

2. Responsive luminescence of metal/polymer hybrids

Changes in luminescent properties of metal/polymer hybrids are among the most direct outcomes when hybridizing metals and polymers. Lanthanides, as an example, with interesting *d-f* excitation, enable intense and sharp metal-centered luminescence (including fluorescence and phosphorescence) to cover entire range of UV and visible spectra.^{35, 36} When incorporating with sensitizing ligands in the coordination sphere, strong “antenna effect” shows enhancement in emission of lanthanide metals.³⁷ “Antenna effect” refers to lanthanide complexes with light harvesting ligands which usually absorb the light and have the energy transfer to metal ions to enhance lanthanide-centered emission. Therefore, the disruption of M-L coordination, particularly the removal of antenna chromophores in the coordination sphere of lanthanides, will diminish their emission intensity. Given the dynamic nature of coordination, potential reversible luminescence switch “ON/OFF” can be designed in response to external stimuli, *e.g.*, temperature, light, pH, electrical field, ionic strength and mechanical forces, under which the coordination can dissociate and then reversibly reform. Alternatively, organic polymers with fluorophores also show intriguing responsiveness upon binding with metals. For example, when coordinating with late transition metals, the charge transfer

from ligands to metals potentially leads to phosphorescence or fluorescence quenching in some cases.^{38, 39} Incorporating metals also enhances the charge carrier mobility and changes the photoconductivity of polymers.⁴⁰⁻⁴³ While the change in polymer physical state likely has impacts on the luminescence properties of metals, newly reversible responsiveness of the luminescence

properties of these hybrids could be enabled. Once coupled with the dynamic nature of M-L coordination, the mechanical strength of hybrid materials, *e.g.*, sol-gel⁴⁴ or soft-tough transitions,⁴⁵ potentially show similar and coupled response with the luminescence properties.

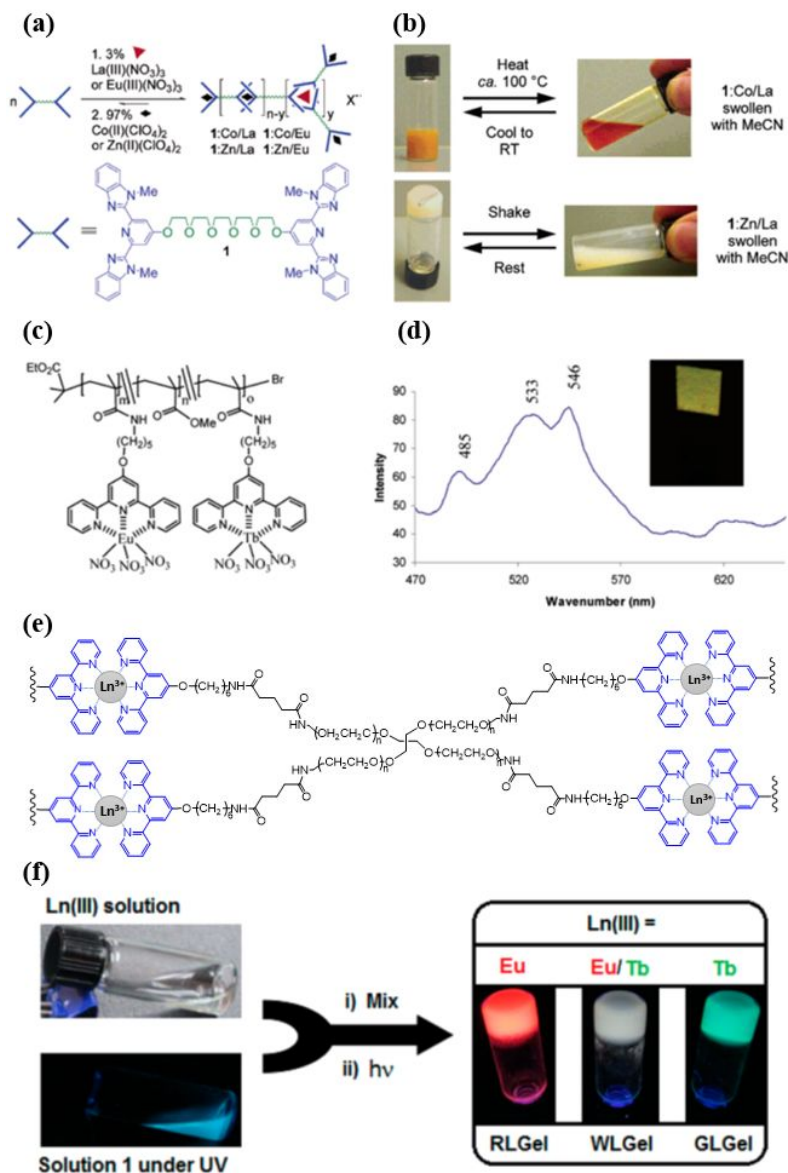


Figure 1. (a) Schematic illustration of the formation of metal-containing supramolecular gels linked by lanthanides and other transition metal ions. (b) Thermo- and mechanoresponsive sol-gel transition of supramolecular gels. (c) Molecular structure of Eu³⁺/Tb³⁺ containing PMMA with terpyridine pendants. (d) Photoluminescence spectrum of the solid film for Eu³⁺/Tb³⁺ ions in PMMA as “alloy” with an excitation wavelength of 350 nm. (e) Chemical structures of the four-arm terpyridine containing PEG and its coordination with metal ions. (f) Pictures of PEG metallogels showing the luminescence under UV light. The excitation wavelength is 365 nm. Figure (a) and (b) reproduced from Ref. 37, copyright 2003 American Chemical Society;³⁷ Figure (c) and (d) reproduced from Ref. 52, copyright 2005 American Chemical Society;⁵² Figure (e) and (f) reproduced from Ref. 22, copyright 2015 American Chemical Society.²²

In case of lanthanide-containing hybrids, the luminescent properties of metals show strong dependence on the coordination. Reversible ON/OFF switch of the emission can be designed using two different methodologies. The first method is called coordination disruption. When coordinated with ligands having strong light

absorption, the antenna effect will enhance the lanthanide emission through a ligand-to-metal energy transfer process. Any stimuli that disrupt the coordination between lanthanides and ligands can weaken the antenna effect and thus reduce the metal-centered luminescence. The second design is based on coordination

competition. The O-H band vibration can quench the fluorescence of lanthanides when it exists in the first coordination sphere.⁴⁶⁻⁴⁸ With competitive binding ligands like water and alcohols, lanthanides favor to bind with O atoms in those ligands, leading to the quenching of lanthanide luminescence. Both methodologies are possible to design reversible switch ON/OFF of the emission of metals due to the dynamic nature of coordination.

2.1 Coordination disruption. One of the early examples from Rowan *et al.* demonstrated the responsive emission of lanthanides to couple with the sol-gel transition of supramolecular gels.^{37, 49} 2,6-Bis(benzimidazolyl)-pyridine (Mebip) as a tridentate ligand has strong absorption around 330 nm.⁵⁰ Capped with a poly(ethylene glycol) (PEG) oligomer (Figure 1a), Mebip can coordinate a number of transition metals. Small early transition metal ions, *e.g.* Co²⁺ or Zn²⁺, are able to bind with two Mebips in a twisted octahedron; while, larger lanthanide ions can coordinate three Mebips. Upon coordination with mixed metals, like Zn²⁺/Eu³⁺ pairs, organogels with strong red emission could be readily formed with the Eu-Mebip coordination as physical cross-linkers. The gelation was resulted from crystallization of the globular particles generated by coordination supramolecules as revealed by X-ray diffraction.⁵¹ Given the dynamic and reversible nature of M-L binding, one would expect reversible sol-gel transition of the organogels in response to various stimuli that disrupt the coordination, including temperatures, changes in pH and mechanic forces. For examples, upon heating to *ca.* 100 °C or shaking, a clear sol-gel transition was seen as a result of the dissociation of Mebip-Ln coordination (Figure 1b). The sol-gel transition was coupled with the luminescent properties of lanthanides, where no emission was seen in the sol state without Mebips in the first coordination sphere. By varying M-L complexation with different stabilities, counterions of metal salts, and possible cores of the ligand-terminated monomers, a wide variety of stimuli-responsive supramolecular gels can be designed.⁴⁴

Compared with supramolecular complexes, lanthanide complexes can be designed in polymer gels or elastomers with high elasticity, stiffness and toughness; while, the luminescence of lanthanides as a probe can monitor the change in polymer networks.^{24, 45, 53-57} Using telechelic copolymers of poly(ethylene-co-butylene) terminated with Mebip (Mw 4,400 g/mol), Weder and coworkers prepared Eu³⁺-containing elastomers with intriguing mechanochemical response due to the dynamic properties of Mebip-Ln binding.⁵⁸ Under ultrasound sonication, the emission intensity of Eu³⁺ ions dropped by 20% as a result of the disruption of Mebip-Ln coordination. The red emission recovered within a few minutes once the sonication stopped. The recovery kinetics of luminescence appeared to be first order, much slower than that in small molecular complexes. As a comparison, polymers containing dipicolinic acid (dpa) did not dissociate under sonication. The mechanical force therefore provides a valuable non-invasive tool to control the dynamic binding of lanthanides in polymer to design smart materials capable of transducing forces into directly readable optical signals.

Sensitizing ligands can be grafted as the polymer side chains to coordinate metals. When coupled with two or more lanthanide metals in polymers, newly stimuli-responsive luminescence can be expected as the imposed steric impact from macromolecular architectures. Using the random copolymers of poly(methyl methacrylate) (PMMA) with terpyridine moieties, emissive

lanthanide metals like Eu³⁺ and Tb³⁺ can be incorporated into polymer films (Figure 1c).⁵² Terpyridine has a UV absorption around 290 nm⁵⁹ and it is a tridentate ligand for a variety of metals. Incorporating Eu³⁺ and Tb³⁺ into terpyridine-containing PMMA films would result in red and green emissive films, respectively. When stoichiometrically mixing Eu³⁺ and Tb³⁺ ions in the polymer at 1:1 (mol), the hybrid films showed a new emission peak at 533 nm that did not exist in individual Eu³⁺ and Tb³⁺-containing films (Figure 1d). As a coordination alloy, the film was yellow emissive (Figure 1d). In contrast, when the two metals were mixed with the same polymer separately, the resultant films containing the two ions had a green emission. The concurrent incorporation of Eu³⁺ and Tb³⁺ ions into the same polymer backbone resulted in an intimate spatial arrangement, possibly bridging bimetallic complex through π - π stacking of terpyridine. This yellow-emissive film showed a reversible thermochromism where an orange emission was observed at 50 °C; while, the yellow emission recovered at room temperature.

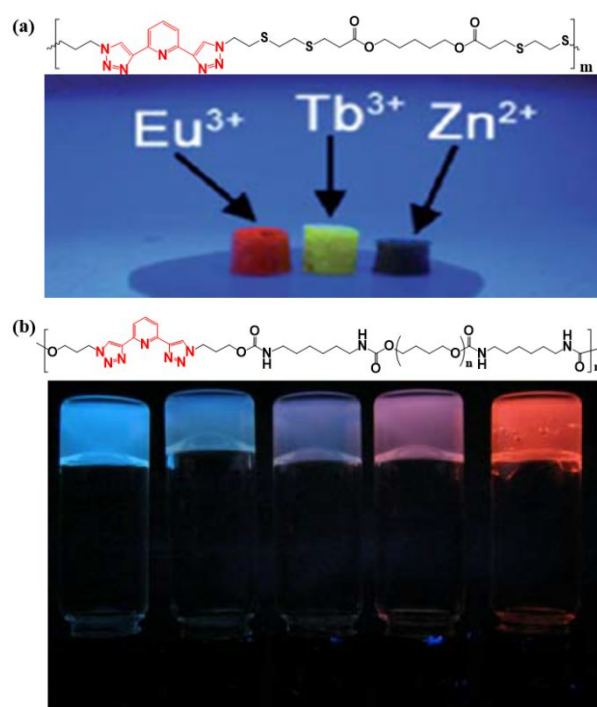


Figure 2. (a) Fluorescent image of the three gels containing different metal ions (Eu:Tb:Zn ratios from left to right are 100:0:0, 0:100:0 and 0:0:100) under UV light (254 nm). The structure of bithiol functionalized polytetrahydrofuran (PTHF) with multiple BTP are shown at the bottom. (b) Image of the gels with different amounts of Zn and Eu ions (from left to right Zn/Eu: 100/0, 75/25, 50/50, 25/75 and 0/100) under 365 nm UV light. The structure of polyurethane containing BTP metal moiety are shown as an inset in this image. Figure (a) reproduced from Ref. 69, copyright 2014 The Royal Society of Chemistry.⁶⁹ Figure (b) reproduced from Ref. 62, copyright 2012 The Royal Society of Chemistry.⁶²

When balancing the emission of several lanthanides, *e.g.*, Eu³⁺ (red), Tb³⁺ (green) and Dy³⁺ (blue), white emitting phosphors can be designed. Compared with other white-light-emitting dyes, lanthanide metal ions are mostly colorless; and therefore, it is possible to design transparent white emitting polymers. In

terpyridine-containing polymers, Tew and coworkers reported the facile production of true white-light emitting phosphors in solution or solid states.⁶⁰ The copolymers containing polystyrene (PS) and terpyridine can incorporate Eu^{3+} , Tb^{3+} and Dy^{3+} simultaneously at any given ratio to tune the emission color. At a molar ratio of 1:1:1.8 ($\text{Eu}^{3+}:\text{Tb}^{3+}:\text{Dy}^{3+}$), true white-light emitting film with a CIE (International Commission on Illumination) coordinate value of (0.31, 0.33). The white-light emitting phosphors can also be designed from two emitters, like the blue-emitting Dy^{3+} -chelated polymer and a red-emitting Ru^{3+} complexes through coupled energy transfer from blue-emitting Dy^{3+} to blue-absorbing Ru^{3+} complexes.⁶¹ As the luminescence of lanthanides is stimuli-responsive, fluorochromic materials can therefore be designed when varying the emission intensity of lanthanides.^{22, 24, 44, 58, 62-68}

The mixing of Eu^{3+} (red) and Tb^{3+} (green) ions in polymers can produce white emissive phosphors as well. Using a terpyridine end-capped four-arm PEG (4-Arm-PEG) (Figure 1e), Holten-Andersen *et al.* developed hybrid organogels consisting of two lanthanide metals,

i.e., Eu^{3+} and Tb^{3+} . The 4-Arm-PEG acted as a perfect physical cross-linker at a terpyridine: Ln molar ratio of 2:1, mol. The gels showed tunable and stimuli-responsive luminescent color. Varying the molar ratio of Eu^{3+} and Tb^{3+} ions led to the formation of organogels with a broad spectrum of emission (Figure 1f). At the Eu -to- Tb molar ratio of 4:96, a white-light emissive gel with a CIE color space (0.30, 0.49) was obtained. Stimuli-responsive properties of those lanthanide-containing gels were explored under mechanical force, chemical vapor, temperature and pH.²² For example, the gel-to-sol transition occurred when subjected to ultrasonication induced mechanical force. Under 5-min sonication, the gel broke down and the white emission changed into blueish as a result of Ln -terpyridine dissociation. Interestingly, the gels showed a nontrivial green-white-red thermochromism under cryogenic conditions. When cycled from -196 to 60 °C, a reversible change in emission color from green to white and eventually to red was observed. The distinctive thermochromism change was caused by the intrinsic energy transfer from Tb^{3+} to Eu^{3+} at a higher temperature.

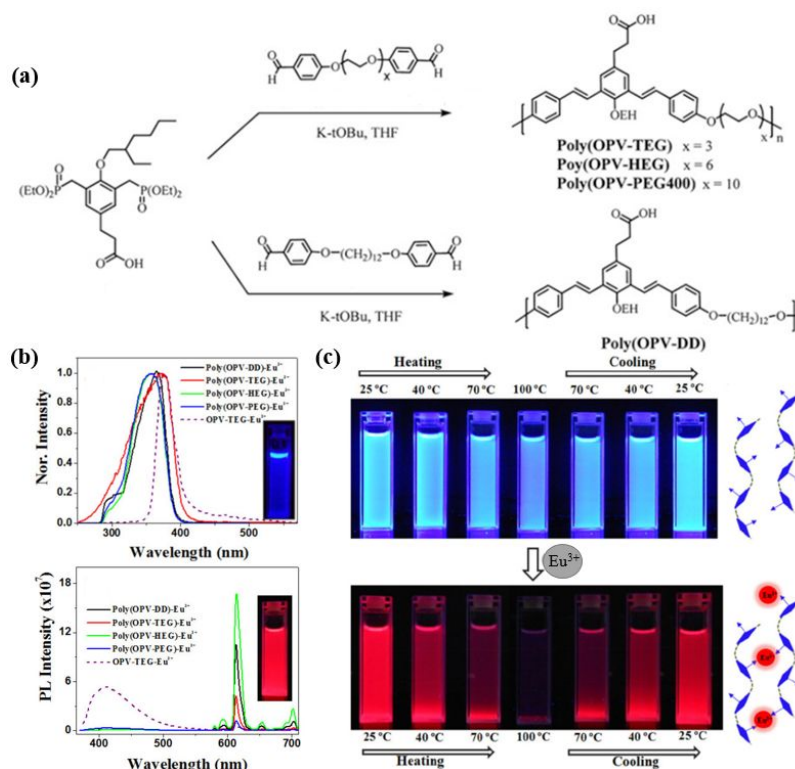


Figure 3. (a) Synthesis of conjugated OPV polymers with binding sites. (b) Excitation (emission wavelength = 615 nm) (upper) and emission (lower) of the polymer and complexes in chlorobenzene. (c) Images of the polymer (upper) and polymer- Eu^{3+} complex (lower) in chlorobenzene at different temperatures. Figures reproduced from Ref. 66, copyright 2013 The Royal Society of Chemistry.⁶⁶

Coordination ligands can be incorporated on polymer backbones in the formation of coordination polymers⁷⁰ or metallopolymers.⁶ Here, coordination polymers refer to inorganic polymers built on metals as linkers on the backbone while metallopolymers have organic polymer backbones coordinated with some metals ions. Using lanthanides in the backbone of copolymers, Weng's group demonstrated two methods to prepare elastic metallo-supramolecular films using 2,6-bis(1,2,3-triazol-4-yl)pyridine (BTP) to bind lanthanides. The first method was to use bispropylene-functionalized BTP that reacted with di-thiol-ended

polytetrahydrofuran (PTHF) via photo-initiated thiol-ene reaction (Figure 2a).⁶⁹ The second method was to incorporate bis-propanol as a chain extender to react with diisocyanate in polyurethane (Figure 2b).⁶² Both polymer could coordinate transition metals, like Eu^{3+} , Tb^{3+} and Zn^{2+} . The BTP ligands bound with Eu^{3+} weakly and the coordination was more dynamic than that of Zn^{2+} . For polyurethane gel containing Eu^{3+} and Zn^{2+} ions, the dynamic properties of those gels were different. With 100% Zn^{2+} (100/0, $\text{Zn}^{2+}:\text{Eu}^{3+}$), the gel-to-sol transition occurred at 140 °C upon heating. The gel-to-sol transition temperature became lower, *ca.* 120 °C and 110 °C for the gels

containing 75% and 100% Eu^{3+} with respect to Zn^{2+} , respectively. Such thermoresponsive sol-gel transition was accompanied with emission quenching of Eu^{3+} where no emission was seen in sol states. As cooling back to ambient temperature, gels were reformed along with the recovery of the Eu^{3+} emission.

When incorporating emissive lanthanides in fluorescent oligophenylenevinylene (OPV, Figure 3a), Balamurugan's group designed carboxylic acid (as the ligand) functionalized π -conjugated polymer- Eu^{3+} ion complexes for thermosensitive luminescent switches in solution and solid states.⁶⁶ When varying the length of oligo(ethylene glycol), the excitation and emission spectra of those OPV polymers were nearly identical with their maximum peaks at 350 nm and 610 nm, respectively. The quantum yields of those polymers were in the range of 0.13-0.27 in solution. When bound with Eu^{3+} ions, excitation energy transfer from π -conjugated OPVs to Eu^{3+} ions were evidenced from the emission quenching of polymers and subsequently produced sharp emission in the range of 570-720 nm from Eu^{3+} ions (Figure 3b). Those OPVs therefore sensitized Eu^{3+} ions as "antennae". The luminescence intensity of Eu^{3+} ions was strongly impacted by temperature in both solution and solid states. The emission intensity of Eu^{3+} ions slowly decreases with increasing temperature. Upon heating to 100 °C, the red emission from Eu^{3+} ions was completely shut down, as a result of the dissociation of the π -conjugated OPV- Eu^{3+} coordination at high temperatures (Figure 3c). The thermosensitivity of those luminescent hybrids had a dependence on the polymer structures. With a longer length of oligo(ethylene glycol), higher breakdown temperatures at which the change in luminescence became active and higher luminescence contrasts were observed.

2.2 Coordination competition. It is challenging to have lanthanides based luminescent hydrogels with intensive emission and high mechanical strength. One of the critical reasons is the hydration of lanthanides ions. Water can bind with emissive lanthanides in their first coordination sphere; then the O-H vibration as an oscillator can quench the luminescence of lanthanides.⁴⁶ The weak binding motifs to lanthanides, like some of the monodentate or bidentate N ligands, can be disrupted by water. For example, there are numerous examples to use molecular Eu^{3+} complexes to pick up the trace amount of water from organic solvents as a means to detect water qualitatively since water quenches the emission of Eu^{3+} .^{45, 71-73} Water can even displace a strong 'tripod' ligand like tris(2-pyridylmethyl) amine.⁷⁴ Therefore only with some ligands, the luminescent lanthanides can be used under aqueous conditions.^{75, 76} In the presence of strong binding motifs in polymers, it is possible to directly have luminescent lanthanides in water.⁷⁷⁻⁷⁹

Our group designed Eu -containing polymer hydrogels that have fast self-healing and tunable fluorochromic properties in response to multiple stimuli.²³ We used a strong ligand iminodiacetate (IDA) as binding motifs to coordinate Eu^{3+} ions that further acted as cross-linkers to prepare polymer hydrogels. IDA is known to have a large binding constant (K_b , the rate constant ratio of coordination on to off, $K_b = k_{\text{on}}/k_{\text{off}}$) to various metals,⁸⁰ while large lanthanide ions can coordinate with three to four IDA ligands simultaneously (Figure 4a). Using copolymers of poly(N,N-dimethylacrylamide-co-3-iminodiacetate-2-hydroxypropylmethacrylate) (P(DMA₂₉₀-co-IDHPMA₉₆)), the formation of Ln-IDA is effectively to exclude water

from the coordination sphere of Eu^{3+} ions in the presence of excess IDA ligands in polymers. When adding Eu^{3+} ions to the polymer, a clear sol-gel transition was observed even at a low Eu content, e.g., the ratio $\text{Eu}:\text{IDA}$ of 1/7, mol. As resultant Eu^{3+} -containing hydrogels showed typical red emission of Eu^{3+} complexes. The emission of Eu^{3+} ions was not strong compared with those antenna-type ligands. Since IDA is a tridentate ligand with deprotonated carboxylic acids and one tertiary amine, the changes in pH can modulate the coordination strength of IDA with Eu^{3+} . Under the acidic condition, the protonation of the two acetates and the amine led to the dissociation of Eu -IDA. In the absence of IDA, the hydration also quenched the emission of Eu^{3+} ions. Therefore, those Eu -containing hydrogels underwent a reversible gel-sol transition along with switchable luminescence of Eu^{3+} ions in response to the change of pH as shown in Figure 4. Other small transition metal ions, like Fe^{3+} , Zn^{2+} and Cu^{2+} , can be used as competitive ligands to weaken the binding of Eu -IDA. For smaller ions, e.g., Fe^{3+} , Zn^{2+} and Cu^{2+} , the binding pocket of IDA fits better with one ion. When adding smaller ions in those Eu -containing hydrogels, similar sol-gel transition could be observed. For example, with a low concentration of Fe^{3+} , ~4 mM, the emission of Eu could be completely quenched. Similarly, heating, sonication and mechanical force could induce gel-to-sol transition of Eu -containing hydrogels. These multistimuli-responsive fluorochromic hydrogels possibly can be used in conjugation with a fluorophore that are not stimuli-responsive. High contrast change of the emission color therefore can be gained for those hybrid materials.^{24, 64, 81} For example, when coupled with green emissive fluorescein, Eu -containing polymers can vary their emission color from white to green where the red emission of Eu^{3+} is switchable in response to stimuli.²⁴ Such stimuli-responsiveness illustrates a new method to make smart optical materials, particularly for the applications in biological sensors where multistimuli responsiveness is required.^{35, 82-89}

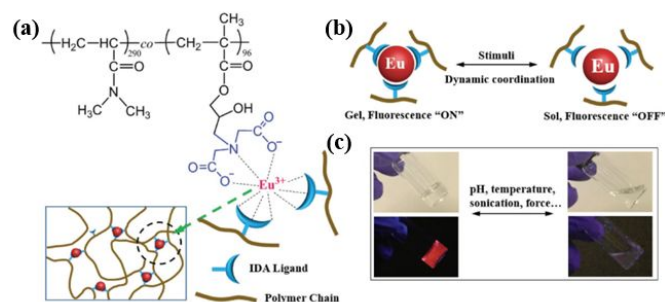


Figure 4. (a) Chemical structure of IDA containing polymers and the cross-linking with Eu^{3+} ions. (b) The scheme to show the sol-gel transition and luminescence ON/OFF of Eu^{3+} containing polymer. (c) Digital pictures to show sol-gel transition and fluorescence ON-OFF with external stimuli. Figures reproduced from Ref. 23, copyright 2018 Wiley VCH.²³

Control of lanthanide luminescence can be coupled with other luminescent materials, like carbon dots (CDs).⁶⁴ When varying the ratio of RGB emitters, one can fabricate white-light emitting phosphors as aforementioned. In addition, Holten-Andersen's group designed mechanochromic polymer films by the physical separation of fluorophores in a layered film.²⁵ Using CDs and lanthanide ions as the emitting species in the top and bottom layers of polymer films,

the top CD layer can act not only as a blue luminescent emitter but also as a UV absorber along with a non-luminescent quencher, 2-(4-benzoyl-3-hydroxyphenoxy)ethyl acrylate (BHEA), for lanthanides. The thickness of the top layer, upon the mechanical stretching, would decrease by the Poisson's effect, resulting in enhanced transmittance of light to the bottom layer where the luminescence of lanthanide was turned ON. Such mechanochromism can be tuned simply by changing the concentrations of CD or BHEA in the top-layer. These mechanochromic polymers have been demonstrated to be useful in pressure and contact force sensing as well as material-based encryption devices.

Other than lanthanides, hybridization of other transition metals in polymers possibly endows interesting stimuli-responsive luminescent properties. Such responsiveness is twofold. On one hand, upon the coordination of metals, fluorophores show fluorescence quenching or enhancement.⁹⁰⁻⁹² This mechanism has been often used in molecular systems for metal cations detection where fluorescent molecules alter their emission with the metal coordination. An obvious case is the charge or electron transfer from fluorophores to paramagnetic metal cations, like Cu^{2+} and Hg^{2+} , leading to the fluorescence quenching.^{93, 94} When incorporating those fluorophores in polymers, signal amplification through large conjugation systems could improve the sensitivity of those sensors.⁹⁵ On the other hand, adding metals can populate triplet states. Triplet emitters are known to efficiently enhance the light-emitting quantum yield,^{96,97} for example in electroluminescence theoretically up to 100% efficiency. Although the details on the mechanism of the metal-ligand charge transfer (MLCT) will not be discussed here, the add-in polymer can endow interesting responsiveness to those luminescent hybrids. In particular, the triplet state of those metal-containing polymers shows responsive phosphorescence.^{98,99}

Other metal cations like Pt^{2+} , Ir^{2+} and Au^{+} can also show MLCTs and enable phosphorescence^{97, 100} in metal-polymer hybrids. For instance, when simply coordinating with poly(4-vinylpyridine) (P4VP), $\text{Au}(\text{C}_6\text{F}_5)^+$ presents strong green emission; while both P4VP and $\text{Au}(\text{C}_6\text{F}_5)^+$ are non-emissive.¹⁰⁰ Although soft Au^{+} and hard N ligands are not incompatible, P4VP could enhance the formation of aurophilic interaction in the form of $\text{Au}(\text{I})\cdots\text{Au}(\text{I})$ both intra- and interchain. The hybrids have a photoluminescence quantum yield of 63%. In solid state, those metal-polymer hybrids showed reversible mechanochromic luminescence between green and yellow-green emissions.¹⁰¹

3. Self-healable metal/polymer hybrids

Self-healable or self-repairable materials can repair themselves upon mechanical damages. The most obvious example is the skin that undergoes self-healing upon minor cuts. For synthetic materials, similar healing properties would improve the lifetime of materials, which is of particular importance for cross-linked polymers, like rubbers. Self-healable polymers are usually built with dynamic bonds that can be broken and reformed reversibly.¹⁰²⁻¹⁰⁵ Those dynamic bonds can be either covalent, like dynamic covalent bonds,^{106, 107} or

non-covalent, like hydrogen bonding,^{108, 109} π - π stacking,¹¹⁰ hydrophobic interaction,¹¹¹⁻¹¹³ and coordination.¹¹⁴⁻¹¹⁷ Most of those dynamic bonds relies on the design of well-defined molecular structures and their interactions are not changeable once the synthesis of polymers is fixed. In other words, to vary the strength of those covalent or non-covalent interaction, new synthesis is usually needed. As a comparison, coordination is among the most feasible to vary interactions used in self-healable polymers. The choose of different metals can lead to the possible changes of on-demand M-L coordination strength in a broad range.

Coordination is one of the most promising non-covalent interaction for the design of self-healable polymers.¹¹⁸ First of all, metal-ligand coordination is highly tunable in term of those binding strength as mentioned. The common binding motifs, such as N and O, vary their coordination affinity or the K_b .¹¹⁹ For examples, pyridine- or phenol-containing ligands show tunable binding affinity to metals in response to pH. The deprotonated forms of pyridines and phenolates are usually strong ligands to transition metals; while their protonated forms are fairly weak. The change in binding affinity plays a determining role in the polymer chain dynamics that controls the chain diffusion and eventually self-healing efficiency. Second, metal-ligand coordination is strong to prepare mechanically stiff polymers. In the example of ferric-catechol complexes, the K_b is in the range of 10^{10} to 10^{40} L mol^{-1} depending on the pH.¹²³ The large K_b results in the formation of strong binding close to covalent bonds. Some metal ions also have large coordination numbers²³ or form nanoclusters¹²⁴ to create high cross-linking density. Lastly, metal endows new functionalities not existing in organic polymers, like luminescence and redox properties.¹²⁵ Taking $\text{Fe}^{3+}/\text{Fe}^{2+}$ as an example, citrate can reduce Fe^{3+} to Fe^{2+} in the presence of UV light.¹²⁶ In the presence of hydrophilic ionic polymers like poly(acrylic acid) (PAA), Fe^{3+} can bind three carboxylates while Fe^{2+} only binds to two carboxylates. When reducing Fe^{3+} to Fe^{2+} , lowering cross-linking density would induce a clear gel-sol transition of PAA solution. It is also possible to design photolabile coordination that endows the light responsiveness to metal/polymer hybrids.¹²⁷⁻¹²⁹

3.1 Bio-related self-healing (Fe^{3+} and Ca^{2+}). In bio-related self-healing applications, the mostly commonly used metal cations are Fe^{3+} and Ca^{2+} .^{26, 118, 130-137} Fe^{3+} -catechol coordination has been identified from the byssal threads of mussels.^{133, 134, 138-140} The byssus contains a protein family rich in tyrosinases which can be converted to catechols through hydroxylation. Abundant catechols can bind a variety of metal ions in the minerals. The K_b is as large as 10^{40} L mol^{-1} .^{27, 123} The tris- and bis-catechol- Fe^{3+} complexes are fairly stable. The single molecule tensile test shows that the rupture force to break catechol- Fe^{3+} binding is 0.8 nN (Figure 5a), comparable to that of a covalent bond, ~ 2.0 nN.¹¹⁸ More importantly, the metal-catechol complexes can reform upon breakage and such dynamic property enables the self-healing of mussel byssal threads.^{131, 141, 142} There have been a large volume of studies on bioinspired coordination Fe^{3+} -catechol to design hybrids with excellent mechanical strength and self-healing capability.

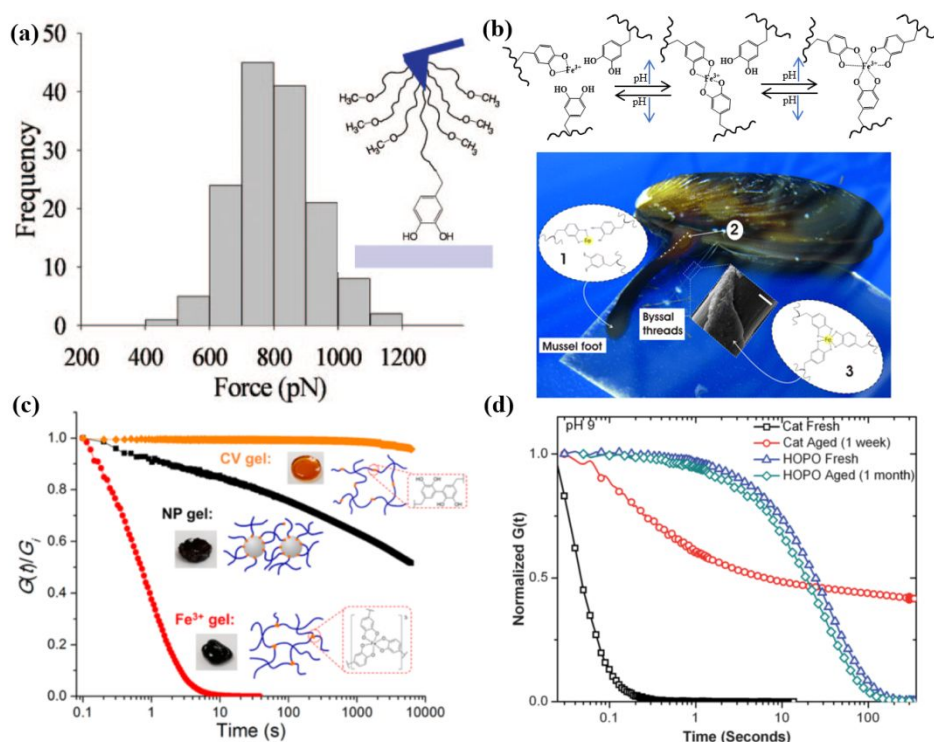


Figure 5. (a) The plot of frequency versus pull out force for he dopa to metal surface. (b) The cross-linking mussel inspired Fe³⁺-catechol containing polymers and their pH responsive Fe³⁺-catechol coordination. (c) Step strain relaxation time of intercatechol covalent crosslinking (CV) gel, Fe₃O₄ nanoparticle gel and Fe³⁺-catechol crosslinked gel. (d) Relaxation time test to characterize the stability of catechol and HOPO hydrogel. Figure (a) Reproduced from Ref. 118, copyright (2006) National Academy of Sciences, U.S.A.;¹¹⁸ Figure (b) Reproduced from Ref. 27;²⁷ Figure (c) Reproduced from Ref. 119, copyright 2016 American Chemical Society;¹¹⁹ Figure (d) Reproduced from Ref. 120, copyright 2013 The Royal Society of Chemistry.¹²⁰

The binding strength and coordination number of Fe³⁺-catechol complexes increase with pH,^{135, 143, 144} although it is possible to form hydroxides under strong alkaline conditions. Waite's group has designed dynamic materials in the forms of hydrogels and elastic films using catechol-Fe³⁺ coordination. Using 4-arm PEG terminated with a catechol at each arm, they demonstrated the self-healing polymer hydrogels with pH-controlled Fe³⁺-catechol binding strength.²⁷ The binding stoichiometry of Fe³⁺-catechol was adjusted by pH through the de-protonation of catechols (Figure 5b). At pH ≤ 5, mono-catechol-Fe³⁺ complex was dominant and it did not cause the cross-linking of the polymer. A green/blue fluid was observed. When raising pH to ~8 at which the bis- or tris-catechol-Fe³⁺ complexes formed, a sticky purple gel was obtained. At pH ~12, tris-catechol-Fe³⁺ was favorable to result in the formation of a red elastic gel. The hydrogels cross-linked Fe³⁺-catechol were self-healable; while, covalently cross-linked hydrogels by NaIO₄-induced oxidation of catechol were not healable.

When using polymeric ligands to bind Fe³⁺ ions, fast gelation usually results in heterogeneous polymeric networks and defective coordination. This often results in mechanically weak hydrogels. One possible solution is to pre-form the coordination complexes prior to polymerizations. For example, polymerizable ligands, like dopamine methacrylamide, chelated with Fe³⁺ ions first.¹⁴⁵ The further polymerization could lead to the formation of dense networks with high mechanic strength without decreasing self-healing efficiency. Dopamine with a similar catechol group could bind with FeCl₃ at pH from 8-10. The formed bis- or tris-catechol-Fe³⁺ complexes had

distinct absorption features. Bis-catechol-Fe³⁺ complexes formed at pH 8 had a maximum absorption peak at 535 nm; while the tris-catechol-Fe³⁺ complexes formed at pH 10 was at 467 nm. At both pHs, it allowed a maximum use of coordination between catechol and Fe³⁺ to decrease the coordination defects. After photopolymerization, highly elastic hydrogels could be yielded. With tris-catechol-Fe³⁺ complexes, the hydrogels had a strain of 1000% at break in a tensile test; and that of the hydrogels with bis-catechol-Fe³⁺ complexes was 800%. Both hydrogels were self-healable within 20 min. After healing The maximum strain of 800% was achieved before the rupture for the hydrogels with tri-catechol-Fe³⁺ complexes.

There are a number of studies on balancing the self-healing efficiency and the mechanical strength of hydrogels formed by catechol-Fe³⁺ complexation. For example, instead of Fe³⁺ ions, Fe₃O₄ nanoparticles can bind with catechol as well, while the network formed by catechol-Fe₃O₄ complexation shows completely different relaxation mechanics.¹¹⁹ With nanoparticles as cross-linkers, the stress relaxation was much slower where there were orders of magnitude more chains involved (Figure 5c). In addition, Fe³⁺ is a strong oxidant and it can oxidize catechol in air thus chemically cross-link hydrogels. Through modifying catechol with strong electron-withdrawing groups on the aromatic ring, the oxidation of catechol can be significantly slowed down. For example, Waite's group designed catechol derivatives, e.g., 4-nitrocatechol and 3-hydroxy-4-pyridinone (HOPO) to bind Fe³⁺ ions.¹²⁰ The hydrogels made from

HOPO-Fe³⁺ complexes showed long-term stability in months without changing their rheological and dynamic characters (Figure 5d).

Another example of bio-related metal ion for self-healing applications is Ca²⁺. Ca²⁺ as an essential metal in biology is multi-functional, such as signal transduction, enzymes and biomineralization.¹⁴⁶ Early studies in alginate gels suggested that divalent Ca²⁺ ions interacted electrostatically with carboxylates of alginate to form hydrogels.¹⁴⁷⁻¹⁴⁹ Those biocompatible hydrogels are not toxic for proteins and cells and they have been used for immobilization of enzymes and cells. Bisphosphate shows high binding affinity to Ca²⁺ ions or other Ca²⁺-containing nanoparticles as inspired by hydroxyapatite in living bones.¹⁵⁰⁻¹⁵² Using polysaccharide hyaluronic acid (HA), bisphosphate ligands can be introduced through EDC [1-ethyl-3-(3-dimethylaminopropyl)carbodiimide] coupling. Ca²⁺ ions can cross-link through the binding with bisphosphate to form self-healable hydrogels. Nevertheless, the binding or the electrostatic interaction of alkaline metals with ligands is fairly weak. The mechanical strength of those hybrid gels is often weak.

3.2 Other metals in self-healing. In terms of the network strength, lanthanides are among the best choice of metals given their large radius and coordination number. They are able to bind 9-12 ligands per metal ions, possibly improving the mechanical strength of hybrids. Bao and co-workers designed an Eu³⁺-containing polyurethane elastomers with β -diketone binding motifs (Figure 6a).⁵³ Using natural produced curcumin, copolymerization with isophorone diisocyanate, poly(tetramethylene ether glycol) and 1,4-butanediol yielded the polyurethane with diketone on the backbone. The addition of Eu³⁺ could improve moduli close to two orders of magnitude at low frequency. When the molar ratio of β -diketone to Eu³⁺ reached 3:1 (mol), the tensile strength of hybrid elastomer reached 1.8 MPa with 900% strain at break. In the meanwhile, there was no obvious increase in tensile strength with other metals, like Cu²⁺.⁵³ Eu³⁺-containing polyurethane elastomers showed spontaneous self-healing at room temperature. The healing efficiency estimated from the restore of tensile strength reached to 98% after 48 h.

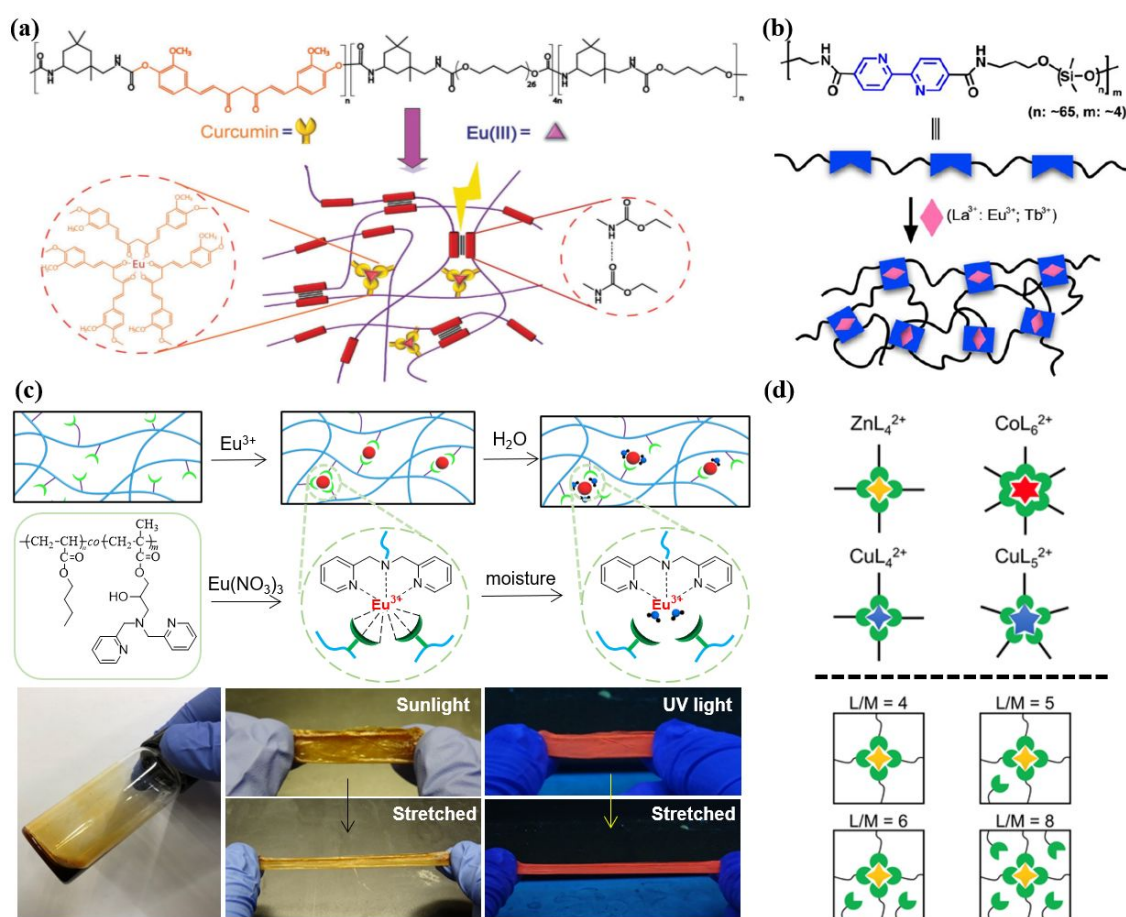


Figure 6. (a) The scheme to show the structure of an Eu³⁺-containing polyurethane elastomers with β -diketone binding motifs; (b) The synthesis process to prepare bipyridine containing polymer and preparation of metal containing elastomer; the bottom scheme illustrate the proposed ligand and counter ion effects. (c) The mechanism of using moisture to control Eu-DPA coordination in $P(nBA-co-GMADPA)$. Pictures showing the pristine state of $P(nBA-co-GMADPA)$ and self-standing film under sunlight or under UV light; (d) The imidazole containing polymer coordinated with different transition metals and the topology effects to mechanical properties; Figure (a) Reproduced from Ref. 153, copyright 2019 Wiley VCH;¹⁵³ Figure (b) Reproduced from Ref. 154, copyright 2017 Wiley VCH.¹⁵⁴; Figure (c) Reproduced from Ref. 45, copyright 2020 The Royal Society of Chemistry;⁴⁵ Figure (d) Reproduced from Ref. 155, copyright 2016 American Chemical Society;¹⁵⁵

ARTICLE

The choice of the counterions seems to play an important role in self-healing efficiency as well. Using bipyridine-containing polydimethylsiloxane (PDMS, Figure 6b), Bao's group showed the importance of counterions on the self-healing ability of hybrid films.¹⁵⁴ Different counterions like trifluoromethanesulfonate (OTf), nitrate (NO₃⁻) for Eu³⁺/Tb³⁺ were compared parallelly on chain mobility and self-healing behavior under room temperature. Triflate lanthanide salts were found to be stronger cross-linker and improve toughness and elasticity. The PDMS film crosslinked by Eu³⁺/Tb³⁺ with OTf showed healing efficiency >90% while Eu(NO₃)₃ and Tb(NO₃)₃ containing film are < 20%. Small angle X-Ray scattering (SAXS) suggested that the film with lanthanide triflate increased the domain size compared to that of the elastomer having lanthanide nitrate. This enhanced chain mobility and resulted in the improvement of healing efficiency.

Although high cross-linking density improves the mechanical strength of hybrid films, this shows great impact on the chain dynamics. There is a trade-off between the chain dynamic and the mechanical strength of hybrid films. With lanthanides, one possible solution is to use competitive molecular ligands, such as water, to trigger fast self-healing; and then, competitive ligands can be removed to restore the mechanical properties. Our group recently designed an Eu³⁺-containing elastomer consisting of poly(*n*-butyl acrylate) (PnBA) incorporated with 2-hydroxy-3-dipicolylamino methacrylate (GMADPA) (Figure 6c).⁴⁵ With 15 mol% of GMADPA, the copolymer with a low Eu-to-DPA ratio of 1:7 formed elastic and self-standing films. The film was stretchable and red-emissive. GMADPA has dipicolylamine moieties as a tridentate ligand with three N atoms to bind Eu³⁺ ions. However, water as a preferred ligand for Eu³⁺ can compete with dipicolylamine. In the presence of trace amount of water, the disruption of Eu³⁺-DPA complexes was seen, leading to, i) significant luminescence quenching of Eu³⁺ ions and ii) lowering the moduli of the hybrid film. The self-healing efficiency of the hybrid film was improved by roughly 100 times in the presence of moisture; while, the mechanical robustness could be recovered after removal of water.

M-L coordination dynamics can also be varied by other stimuli, *e.g.*, light. For Ru complexes, ligand substitution and exchange can be triggered by the change of ligand field in photoexcited states.¹⁵⁶ For example, in [Ru(terpy)(phen)(L)]²⁺ (terpy: 2,2',6',2''-terpyridine; phen: 1,10-phenanthroline; and L is a thioether or other weak ligands), the weak L ligand can be photocleaved and replaced by water upon excited by light;¹⁵⁷ while, the unstable Ru-H₂O can return to the thermodynamic stable Ru-thioether form in dark. Wu and coworker demonstrated the use of photocleavable Ru-thioether binding in light-triggered fast self-healing gels.¹⁵⁸ Using polymerizable pentacoordinated Ru complexes with (2-(2-(2-(methylthio)ethoxy)ethoxy)ethyl acrylate and N-hydroxyethyl acrylamide, organohydrogels could be prepared in H₂O/glycerol

mixtures with a concentration of Ru complexes ~1 mol% relative to N-hydroxyethyl acrylamide. Such organohydrogels showed interesting light-triggered sol-gel transition. Upon exposure to green light (530 nm, 10 mW cm⁻²), organohydrogels became fluidic after 5 min irradiation as a result of the cleavage of Ru-thioether cross-linkers. The gel state could be recovered when storing the liquid in dark after 25 min. The organohydrogels allowed the reversible sol-gel transition to occur even at -20 °C. Those organohydrogels were healable in similar timeframe as triggered by light irradiation. Light as a trigger provides spatial control of the healing region where the gel-to-sol transition could be induced locally for rapid recovery.

Other than coordination strength, coordination geometry of transition metals also play a role in the self-healing behaviors of hybrid films.¹⁵⁹⁻¹⁷⁰ The coordination geometry of metals determines the number of ligands and further chain dynamics which are tunable by the chemical nature of ligands.^{28, 165, 169, 171, 172} The mechanical properties and self-healing behaviors of hybrid films were influenced by the choice of metals as demonstrated by Guan's group.¹⁵⁵ Using imidazole-containing brush polymers of PnBA and polystyrene (PS), three different metals, *i.e.*, Co²⁺, Zn²⁺ and Cu²⁺ with the similar ionic radius and electrostatic charge, were incorporated to investigate their impact on solution and bulk film properties (Figure 6d). Zn²⁺ and Cu²⁺ ions showed more dynamic behavior where brush polymers had no changes in viscosity and elasticity with low metal loading (metal-to-ligand ratio < 1:4); but there was a sharp transition with further increase of metal loading. For Co²⁺, there was a proportional increase in viscosity of polymer solutions and melts. The tetrahedral complexes, such as Cu²⁺ and Zn²⁺ with imidazole, were thought to have a fast ligand exchange, compared to that of octahedral Co²⁺ where the ligand exchange rate was independent on the concentration of free imidazole. The large difference in coordination geometry and dynamics had similar impact on self-healing efficiency. Zn²⁺-containing brush polymers showed 90% healing after 3 h,¹⁷³ while it was less than 30% for Co²⁺-containing polymers. The ligand exchange dynamics therefore determines the diffusion rate of polymer chains which dominates the self-healing efficiency.¹⁵⁵ Similarly, in bipyridine-containing PDMS, Zn²⁺ showed a fast self-healing compared to Fe²⁺.¹¹⁶

M-L coordination alone as physical cross-linker in polymers usually is still too weak to yield self-healing materials with high mechanical strength. Another possible solution is to combine M-L coordination with other non-covalent interactions like hydrogen bonding and hydrophobic interaction. The formation of two networks can significantly improve the mechanical strength of polymers (see Section 4). Since both networks are formed by non-covalent interactions, those hybrid polymers are self-healable. For example, bi-functional acrylate, 2-(3-(3-imidazolylpropyl)ureido)ethyl acrylate (IUA), is polymerizable. It provides hydrogen bonds through ureido and M-L coordination

through imidazole. Using the random copolymers with PnBA, Zn²⁺-imidazole complexation could improve the tensile strength by ~40 times.²⁸ The film was healable upon heating up to 88% after 48 h. Yamaguchi and coworkers prepared copolymers of poly(δ -valerolactone)-poly(lactic acid) (PVL-PLA) containing the ligands of 2,2-bipyridine and the hydrogen bond sites of 2-ureido-4-pyrimidinone.¹⁷⁴ Three metal ions of Zn²⁺, Co²⁺ and Fe²⁺ could be incorporated into the polymeric networks. The films with double networks had a high toughness, *e.g.*, ~85 MJ·m⁻³ of Fe²⁺-containing films, 3.5-fold higher than that of the metal-free films. The hybrid films also showed a reasonable healing efficiency up to 77% after annealing at 50 °C for 30 min.

4. Tough elastic metal/polymer hybrids

Toughness defined as the amount of energy dissipation before the broken of a material is an important measurement of the fracture-resistance of a material. Previous studies on elastic polymers including hydrogels and elastomers suggest that, when building two interpenetrated, covalently cross-linked networks in the elastic polymers, the toughness of elastic polymer can be improved significantly.¹⁷⁵⁻¹⁸¹ In these interpenetrated or double-network polymers, the two different networks are very different from each other in terms of the strength.^{176, 178} The one network is usually weaker (low fracture stress, dense network) and more brittle (low extensibility) than those of the other network. Upon stretching, the weaker network ruptures first, while the second stretchable network retains the integrity of the elastic polymers. The rupture of the weaker network dissipates a large amount of energy (*i.e.*, the work done by stretching) to avoid any damage of the second network. This endows interpenetrated or double-network polymers with high toughness. An alternative design to toughen those elastic materials is to build the weak networks with non-covalent interactions.^{24, 182-189} As such, the stronger network, *e.g.*, made from covalent cross-linking, mainly contributes to the mechanical robustness (high modulus); while the other network, *e.g.*, made from non-covalent cross-linking, dissipates energy through reversible dissociation upon deformation (high elasticity).¹⁹⁰ In the stress-strain curves, tough materials usually show a distant yield region where the weak network starts to break down and the loose but strong network retains the integrity of polymers. When both networks are made with chemical cross-links, the loss of such toughness is permanent because the disrupted network is not recoverable. If the brittle network is built with non-covalent interaction, the toughness of those elastic polymers is recoverable upon the reformation of those non-covalent interactions.

Dynamic M-L coordination is among such non-covalent cross-links to build up tough elastic hybrids. The strength of coordination complexes as measured by $\Delta G_{\text{complex}}$ varies from very weakly chelating systems to strongly chelating M-L (> 100 kT) pairs like catechol-Fe³⁺.²⁷ The dynamic cross-links make the brittle network reversible and add-in large energy dissipation. In typical preparation of tough elastic polymers, the weak M-L complexation can be added before the formation of covalent cross-linking in the polymers. Suo and co-workers reported the preparation of tough and highly stretchable hydrogels using chemically cross-linked ionic polymers together with weak ionic interaction.¹⁸² Alginate, as discussed in

previous Section, binds with divalent cation Ca²⁺ through weak coordination/ionic interaction with carboxylate. In polyacrylamide hydrogels, the addition of alginate and calcium sulphate induced a weak physical cross-linking network together with the hydrogen bonds among alginate. After photopolymerization to chemically cross-link acrylamide with N,N-methylenebisacrylamide, highly stretchable and tough hydrogels could be obtained. Despite with 86 wt% of water, the hydrogels could be stretched > 20 times to their initial length with a fracture energy of 8,700 J·m⁻³, while the parent hydrogels of alginates and polyacrylamide only show fracture energy of 10-250 J·m⁻³. The hydrogels were also notch-insensitive and up to 1700% strain at break was seen for the films with notches. When stretching the hydrogels with two networks, the polyacrylamide network formed by chemical cross-links remained intact and the alginate network unzipped gradually. The break of non-covalent interaction of alginate-Ca²⁺ dissipated the energy and the hydrogels showed large hysteresis. The non-covalent binding of alginate-Ca²⁺ could restore and then heal the weak networks as well as the toughness of polymer hydrogels. Such hybrid hydrogels are ideal as a model system to design tough elastic materials and explore mechanisms of deformation and energy dissipation.^{53, 185, 187, 188, 191-197}

The toughness of elastic materials consisting of covalent and non-covalent networks is recoverable since the weak interaction also the non-covalent network is reversible. However, such recovery of toughness is kinetically slow. In the first report from Suo's group, the recovery of toughness was around 74% after 24 h. The immediate cycle of loading/unloading would result much weaker hydrogels. A possible solution is to use dynamic covalent bonds to build up the strong network. Dynamic covalent bonds are strong enough to retain the macroscopic shapes of the films/hydrogels under high strain; while, it endows faster chain kinetics to rezip the non-covalent interaction and to restore the double networks. When combining dynamic covalent cross-links, the tough elastic materials are also self-healable. Ghanian *et al.* demonstrated the tough hydrogels with fast recovery of toughness using the double networks formed by Diels-Alder reaction and alginate-Ca²⁺ binding. For alginate, partial substitution of the carboxyl groups with furan could couple with four-arm PEG-maleimide (4arm-PEG-Mal).¹⁹⁸ Diels-Alder reaction of 4arm-PEG-Mal and alginate occurred under UV-vis irradiation and chemically cross-linked the hydrogels. The toughness of hydrogels was tunable by controlling the substitution degree of furan on alginate. With 20% of furan substitution degree, the hydrogels had a toughness of 136.7 J m⁻³. Such hydrogels had a set of interesting features such as fast self-recoverable toughness and self-healing upon rupture. Even after immediate reloading, the toughness of hydrogels was fully recovered.

Changes in coordination strength possibly improve the mechanical properties of tough elastic hybrids. For example, when using lanthanides in the weak, non-covalent networks, hydrogels are tough, photoluminescent and mechanically strong. Eu³⁺-alginate and polyacrylamide hydrogels had tensile strength of 1 MPa with an energy dissipation of >9,000 kJ·m⁻³ at a maximum strain of 2,000%.¹⁸⁶ In the hydrogels of Eu³⁺-alginate and poly(vinyl alcohol) (PVA), the resultant hydrogels exhibited high mechanical strength as well, *e.g.*, > 7 MPa in compressive strength and 900 kJ·m⁻³ energy dissipation under 400% stretch. In addition, with lanthanide ions,

those hydrogels were strongly photoluminescent and active in antibacterial.¹⁸³ Hong *et al.* have compared the impact of metal cations on the mechanical strength of polyurethane elastomer.¹⁹⁹ With Eu^{3+} ions, the elastomer had a tensile strength of 15.2 MPa at break of 1,053% strain and toughness of 59.1 MPa as the area under stress-strain curve. With Zn^{2+} , the elastomer film had a tensile strength of 9.5 MPa at break of 1,450% strain and toughness of 50.5 MPa. The improvement in the tensile strength and toughness was a result of intermolecular cross-linking by metal cations with larger coordination numbers.

In case of lanthanides, toughness of hybrid films is stimuli-responsive as the coordination of lanthanide ions is responsive to water as discussed previously. When the weak network can be turned ON or OFF, the mechanical behavior is therefore shapeable. In the presence of M-L coordination, the tough elastic mechanics is expected as the coordination dissipates the energy. When further weakening the coordination, the toughness can be removed to form "soft" elastic materials. Our group demonstrated this strategy using dynamic coordination of Eu^{3+} -IDA as a key component to build up the physical cross-linking network in the elastic films consisting of interpenetrated networks. We used chemically cross-linked poly(acrylic acid-co-*n*-butyl acrylate) by ethylene glycol dimethacrylate as the strong network and iminodiacetate-containing

poly(di(ethylene glycol) methyl ether methacrylate) (PMEO₂MA) to coordinate Eu^{3+} ions as the weak network (Figure 7a).²⁴ After removal of solvent, highly elastic films could be prepared. The reversible dissociation and reformation of the Eu^{3+} -IDA complexation could dissipate energy very efficiently. Even with a low content of Eu^{3+} ions (the mole ratio of IDA-to-Eu 7/1), the modulus of the tough polymer film reached 24.3 MPa (Figure 7b), one order of magnitude higher than that of the film without Eu^{3+} ions.²⁴ The energy dissipation of the first cycle reached $>1,500 \text{ kJ}\cdot\text{m}^{-3}$ at 200% strain (Figure 7d). The coordination network underwent fast recovery where $> 900 \text{ kJ}\cdot\text{m}^{-3}$ energy dissipation was seen immediately after reloading. The toughness and photoluminescence were responsive to moisture. Under 80% relative humidity, the hybrid polymer film was "soft" elastic without any yielding point along with the significant weakening of its red emission (Figure 7e and 7f). Both mechanic states and photoluminescence were restored after removing the moisture from the film. The *in situ* dynamic mechanic test indicated the storage modulus of hybrid films decreased with purging moisture and the films showed more significant viscous property. The storage modulus recovered after removing the moisture within 25 min where the elastic solid state could be restored as well.

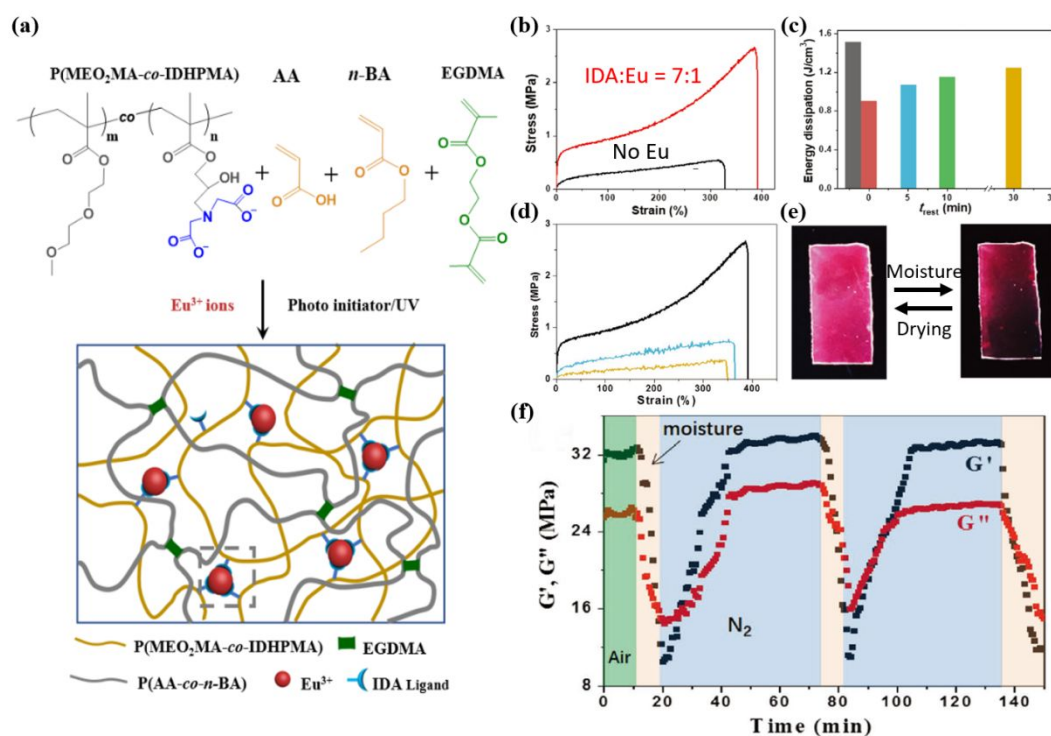


Figure 7. (a) Illustration of the network structure of the IPN tough elastomer. (b) Tensile stress curves of the elastomer without Eu^{3+} ions (black) and Eu^{3+} -containing elastomer (red). (c) Histogram of toughness calculated from cyclic loading with maximum strain of 200%. From left to right denotes the first to fifth cycle. The second to fifth cycle has a rest time (t_{rest}) of 0, 5, 10, 30 min, respectively. (d) Stress-strain curves of the Eu^{3+} -containing polymer films subject to 0 h (black), 1.5 h (blue) and 2.5 h (orange) of moisture at a relative humidity of 80%. (e) Images showing reversible luminescence ON/OFF response of the elastomer film triggered by moisture at room temperature. (f) Moisture-driven switch between elastic solid and viscous fluid states of the elastomer by the dynamic mechanical measurement in a closed chamber alternatively purged with N_2 /water-saturated air. Figures reproduced from Ref. 24, copyright 2019 Wiley VCH.²⁴

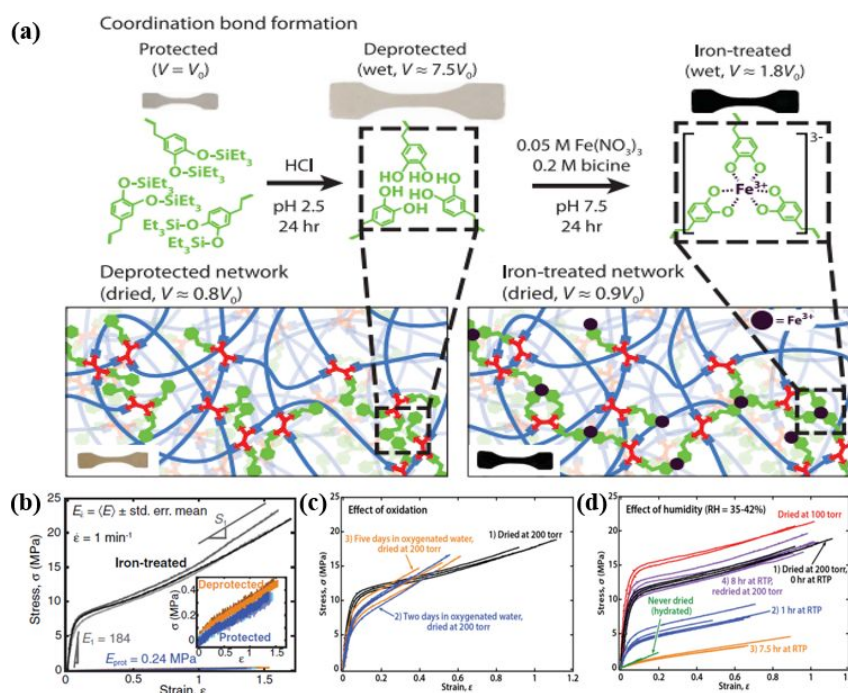


Figure 8. (a) Image to show the protected and deprotected network, the cross-linking network prepared with Fe^{3+} -catechol and the illustration of swelling test specimen during the process. (b) Stress-strain curves of protected (blue), deprotected (orange), and iron-treated samples (grey) with a strain rate of 1 min^{-1} . (c) The effect of oxidation on the mechanical property of the sample. (d) The influence of humidity on the stress-strain relationship of the sample. Figures reproduced from Ref. 136, copyright 2017, Science.¹³⁶

The balance of materials toughness and strength is somewhat similar to those in self-healing. Solely increasing the mechanical strength usually leads to the formation of more brittle and less elastic materials. Valentine and co-workers demonstrated that the use of catecholate- Fe^{3+} coordination could possibly offer a solution to balance the strength and toughness (Figure 8a).¹³⁶ In the amorphous epoxy with loosed chemical cross-links, triscatecholate- Fe^{3+} complexation was designed through mild deprotection under low pH to avoid catechol-catechol oxidative coupling. The triscatecholate- Fe^{3+} formed a stable but dynamic network. With this strategy, the dry elastomer had a Young's modulus of 184 MPa while retaining good stretchable with maximum strain of $\sim 150\%$ was kept (Figure 8b). The polymers with triscatecholate- Fe^{3+} coordination network showed a 58-fold higher tensile strength than the pure polymer; and, the elastic modulus increased by 770-fold after introducing Fe^{3+} ions. As a comparison, the stiffness and extensibility of the tough elastomers were weakened under oxidative conditions and high humidity which swells the Fe^{3+} -rich domains (Figures 8c and d).

There has been a large volume of works on metal-toughen natural and synthetic rubbers.²⁰⁰⁻²⁰³ Most of those rubbers are chemically cross-linked by sulfur or chemicals. Adding in M-L coordination as a sacrificial network could possibly toughen those materials. Guo and co-workers demonstrated that incorporating M-L coordination into rubber enhances the mechanical stiffness as well as the toughness of rubber materials. For example, for the styrene-butadiene rubber containing vinylpyridine, a small amount of Zn^{2+} ions could lead to the improvement of tensile strength and toughness without significant change in elasticity.²⁰² Sacrificial M-L coordination dissipates a large amount of energy which enhances the toughness of the rubber materials.

5. Catalysis using metal/polymer hybrids

While most of synthetic polymers are not catalytically active by themselves except in acid-base hydrolysis, catalytically active metals can be supported on synthetic polymers. Loading expensive metal catalysts on insoluble polymer beads or films offers a valuable way to recycle and recover those catalysts. The rational to use those polymer-supported metal catalysts is to reduce the cost of expensive catalysts and increase their lifetime. There are quite a few excellent reviews with a focus on those polymer-supported metal catalysts.^{8, 204-206} The question of this section we would like to address and summarize is whether synthetic polymers contribute to the catalysis of metals, like catalytic efficiency and selectivity.²⁰⁷ The ideal role of polymers in catalysis is twofold. First of all, synthetic polymers work as the second coordination sphere of metals to control the access of substrates. The early studies on core-functionalized dendrimers suggest that the branched chains of dendrimers can tune the accessibility of metals confined in the core of dendrimers.²⁰⁸⁻²¹⁰ Later examples on stimuli-responsive polymers show that the reversible change in coil-globular confirmation can turn ON/OFF the catalytic activity of metal ions/nanoparticles.²¹¹⁻²¹⁴ Second, polymers provide an "ensemble" environment to metals that varies the local pH, the concentration of protons, hydrophobicity and number of metal sites. The impact of polymer could be different from reactions to reactions; but it is highly engineerable on demand for any given specific reaction.²¹⁵⁻²¹⁷ For example, polymers with multi binding motifs can bring a number of metal sites in one polymer chain with identical coordination chemistry.^{218, 219} Those metal/polymer hybrids show better activity for reactions catalyzed by multimetals cooperatively, as compared to the monomeric coordination metal complexes. In

addition, synthetic polymers as a support offer better stability to metal ions/nanoparticles during reactions, largely increasing the lifetime of hybrid catalysis.^{220, 221}

5.1 Polymer-promoted catalysis. Dendrimers and other branched polymers have historically received numerous interests. Dendrimers with well-defined branched structures offer precise control over the location and number of the active sites. Metal-containing dendrimers usually with multi activate sites on nanosized molecules are considered to bridge the study of homogeneous and heterogeneous catalysis. Depending on the location of metals, there are two different metal-containing dendritic catalysts, including periphery- and core-functionalized dendrimers where the metal sites present on the surface and the core of dendrimers, respectively.²²² Periphery-functionalized dendrimers supports multiple metal sties, possibly promoting their catalytic activity; while, the core-functionalized dendrimers with usually one or two metal sites per molecule offer better spatial control to the metal sites.

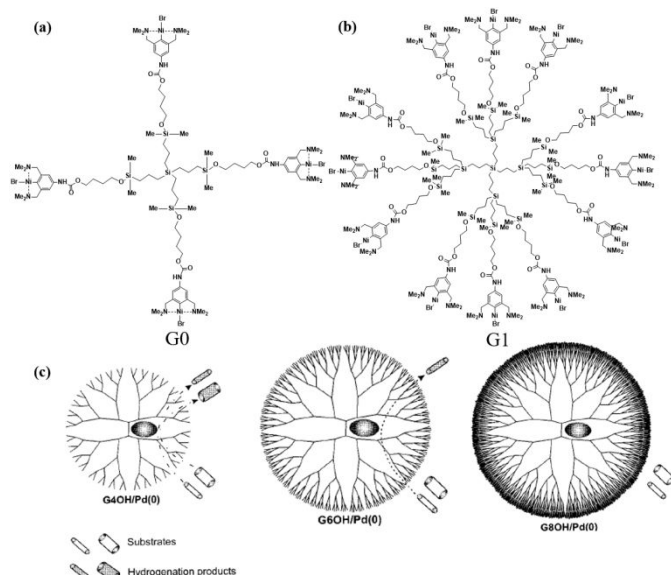


Figure 9. Structure of Ni²⁺-containing dendrimers, (a) G0 (four Ni²⁺ sites) and (b) G1 (twelve Ni²⁺ sites); (c) Scheme to illustrate how the surface crowdedness of dendrimers limits the accessibility of the Pd (0) and catalyst. Figures (a) and (b) redraw from Ref. 223;²²³ Figure (c) reproduced from Ref. 30, copyright 2001 American Chemical Society.³⁰

Using low-generation dendrimers, the periphery-functionalized dendrimers can separate multiple metal sites on the surface of dendrimers that nearly retains the activity of each metal sites. Knapen *et al.* prepared silane dendrimers (G0 and G1) with homogeneous Ni²⁺ sites to catalyze Kharash addition of C=C bonds.²²³ The turnovers per Ni²⁺ site were *ca.* 80% and 70% for of G0 (four Ni²⁺ sites) and G1 (twelve Ni²⁺ sites), respectively, compared to that of mononuclear Ni²⁺ complexes (Figures 9a and b). The dendritic effect on catalytic efficiency usually varies on different reactions. In periphery-functionalized dendrimers, positive dendritic effect is expected when there is a cooperativity between terminal groups. For example, Ouali *et al.* studied the use of Cu-containing dendrimers to catalyze the O- and N-arylation.²²⁴ For the coupling of iodobenzene

and 3,5-dimethylphenol, there was a weak dendritic effect for Cu-containing G1 and G2 catalysts where the yield of diarylether was comparable with monomer Cu catalyst bound with bidentate N-[(1E)-pyridin-2-ylmethylene]-aniline. On the contrary, for the arylation of pyrazole with aryl halides (iodobenzene and bromobenzene), Cu-containing G1 and G2 catalysts had a significant dendritic effect. There was >20-fold higher yield for dendritic Cu catalysts compared to that of the monomeric Cu catalyst. The higher generation dendrimers for both arylations were much more active than monomer Cu catalyst. The dendritic catalysts also show unique kinetic enhancement of 2-3 orders of magnitudes together with polyvalent substrates as demonstrated by Finn and coworkers.²²⁵ Enhanced binding and rolling in polyvalent catalysts and substrates show very interesting dendritic effects on catalysis.

In core-functionalized dendrimers, metal sites are confined by branched molecules that possibly control the accessibility of metal ions.^{30, 208-210} For example, steric crowding imposed by dendrimer periphery control the diffusion rate of substrates dendrimers, thus resulting in different reactivity on metals. Crooks and coworkers demonstrated that Pd nanoclusters (~1.7 nm) encapsulated in poly(amidoamine) (PAMAM) dendrimers showed size-selective hydrogenation of olefins.³⁰ Those tiny nanoclusters were synthesized with hydroxyl-terminated PAMAM dendrimers with different generations G4, G6 and G8. By varying the generations of PAMAM dendrimers, the average distance between terminal hydroxyl group was tunable, *e.g.*, 8.2 Å for G4, 5.4 Å for G6 and 3.2 Å for G8. When increasing the size of substrates, *i.e.*, allyl alcohols, the accessibility became limited as a result of the bulkiness of the dendrimer periphery. There was a clear trend of the Pd catalytic activity correlated to the size of substrates and the generation of dendrimers. The maximum turnover frequency of Pd nanoclusters reached 480 mol H₂ h⁻¹ per mol Pd for the simplest allyl alcohol using Pd in G4. For the same substrate, the turnover frequency of Pd dropped to 120 mol H₂ h⁻¹ per mol Pd using G8. With the Pd in G4, the turnover frequency for 3-methyl-1-penten-3-ol also dropped to 100 mol H₂ h⁻¹ per mol Pd. The surface crowdedness therefore limited the interaction between the metal site and the substrate (Figure 9c).

Once bound with polymers, the availability of metal catalysts is variable by changing physiochemical properties of polymers. Using synthetic polymers as ligands also endows unique responsiveness to the metal catalysts that do not exist in molecular complexes. For examples, thermoresponsive polymers can shift their solubility, known critical solution temperature.²⁰⁶ When bound with metals, those responsive polymers can inverse their solubility to control the metal-substrate binding. Bergbreiter and coworkers showed that thermoresponsive Pluronic block copolymers of poly(ethylene oxide)-*b*-poly(propylene oxide)-*b*-poly(ethylene oxide) (PEO-PPO-PEO) bound with Rh⁺ had anti-Arrhenius reactivity.²¹⁴ Modified by alkyldiphenylphosphine at two ends, PEO-PPO-PEO had a lower critical solution temperature (LCST) around 25 °C. Rh⁺ bound with PEO-PPO-PEO was active when the polymer ligands were water-soluble. At 0 °C, the turnover frequency of 13 mole H₂ h⁻¹ per mole Rh⁺ was received; while, the catalyst was inactive above 25 °C where simply polymer catalysts became insoluble. Similar, the change in polymer chain conformation varies enantioselectivity of bound metals.²²⁶ Single-handed helical poly(quinoxaline-2,3-diyl) showed

assisted electroreduction of CO_2 while preventing proton reduction.²²⁹

There are a few groups reported the outer coordination sphere effect provided by polymeric bases to improve the activity for proton reduction.^{32, 228, 230, 231} The hydrogenase as one type of anaerobic enzymes reduces proton to hydrogen. The $[\text{2Fe-2S}]$ cluster with a $(\mu\text{-S}_2)\text{Fe}_2(\text{CO})_6$ structure can mimic the diiron active sites in hydrogenases. Incorporating the $[\text{2Fe-2S}]$ cluster in water-soluble polymers can resolve solubility and stability of the cluster. Pyun and coworkers designed polymer-grafted $[\text{2Fe-2S}]$ using atom transfer radical polymerization (Figure 11a).²²⁸ Starting with a Br symmetrical initiator prepared from $[\text{2Fe-2S}]$ hydroquinone reacting with α -

bromoisobutryl bromide, methacrylate-based monomers could grow on the $[\text{2Fe-2S}]$ cluster. The cluster grafted with poly(2-dimethylamino) ethyl methacrylate (PDMAEMA) was extremely active to reduce proton with a high current density of $J = 22 \text{ mA cm}^{-2}$ at the reduction peak. According to the results from the Tafel plots, a lower overpotential (0.2 V) comparing to that of the Pt disk could be achieved to reach turnover of 25000 s^{-1} . The high activity was a result of protonated PDMAEMA at pH 7 to enhance the localized proton concentration. When grafting with non-ionic polymers, e.g., poly(oligo(ethylene glycol) methyl ether methacrylate) (POEGMA), the $[\text{2Fe-2S}]$ cluster was inactive to produce hydrogen (Figure 11b).²¹⁷

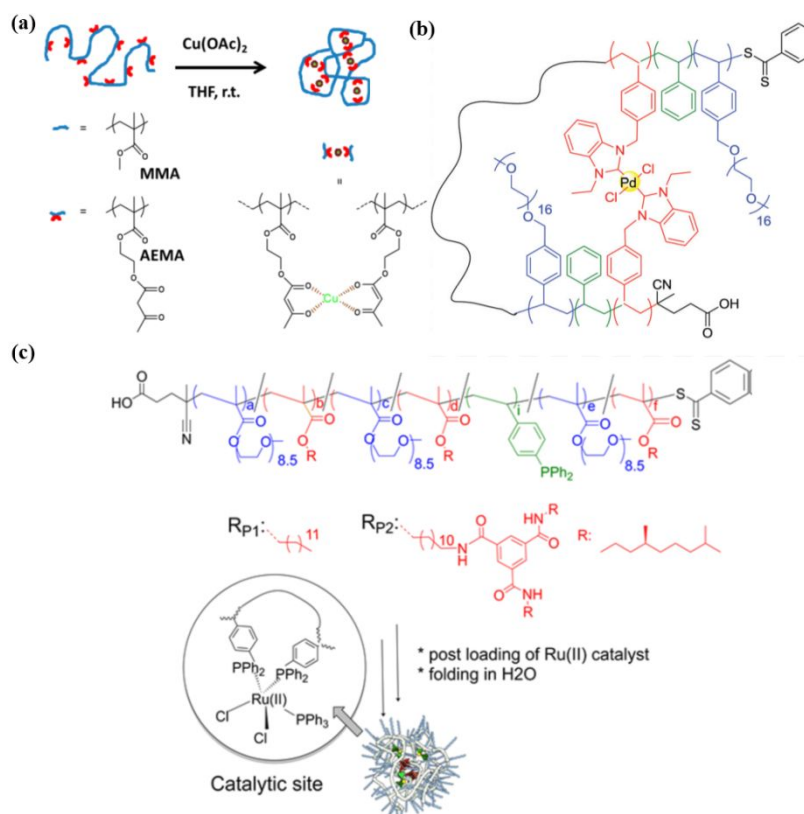


Figure 12. (a) Chemical structure of Cu^{2+} -containing SCNPs. (b) PEG-b-PS SCNPs formed with Pd-NHC coordination. (c) Chemical structure of Ru^{2+} -containing SCNPs driven by BTA intramolecular crosslinking; (c) SCNPs containing phosphine- Pt^{2+} ; Figure (a) reproduced from Ref. 237, copyright 2014 American Chemical Society copyright;²³⁷ Figure (b) reproduced from Ref. 240, copyright 2018 The Royal Society of Chemistry;²⁴⁰ Figure (c) reproduced from Ref. 241, copyright 2015 American Chemical Society.²⁴¹

5.2 Metal-containing single chain nanoparticles (SCNPs). While linear polymers can improve catalytic efficiency of metal ions, the resultant activity of metal ions is still far from that of metalloenzymes. To create more sophisticated outer coordination environments to metal sites, there has been numerous efforts in metal-containing SCNPs. SCNPs are self-collapsed random coils and their sizes are in the range of 5-40 nm, fairly close to that of metalloenzymes. Many intramolecular cross-linking chemistries have been developed in the past, such as covalent coupling, hydrogen bonding, hydrophobic interaction and M-L coordination. Interested readers can find more details in recent review articles.²³²⁻²³⁵ When confined metal sites in SCNPs, there is a higher degree of controllability on outer coordination sphere that is not possible for linear polymers.²³⁶ Other than the advantages of linear polymers,

SCNPs can provide hydrophobic or chiral domains even in water-rich solvents; and SCNPs can possibly confined two or more types of metals for cascade reactions.

Catalytically active metals can be incorporated in SCNPs using M-L coordination as non-covalent cross-linking. Pomposo and coworker designed Cu^{2+} -containing SCNPs using a copolymer of methyl methacrylate (MMA) and 2-(acetoacetoxy)ethyl methacrylate (AEMA) (Figure 12a).²³⁷ Cu^{2+} ions bound with two β -ketoester triggered the self-collapsed of polymer chains. The size of Cu^{2+} -containing SCNPs was around 15 nm. Those hybrid catalysts were very active and highly selective to catalyze the oxidative coupling reaction of acetylenes. Even at a low catalyst loading $\sim 0.5 \text{ mol}\%$ at which $\text{Cu}(\text{OAc})_2$ nor $\text{Cu}(\text{acac})_2$ were inactive, Cu^{2+} -containing SCNPs were highly active ($> 98\%$ yield) of the coupling of propargyl acetate.

Interestingly, Cu^{2+} -containing SCNPs were very selective to propargyl substrates with different molecular sizes. Using a mixture of substrates including propargyl acetate, propargyl benzoate and octyne, Cu^{2+} -containing SCNPs only catalyzed the homocoupling of propargyl acetate. Again, such selectivity did not exist in $\text{Cu}(\text{OAc})_2$ nor $\text{Cu}(\text{acac})_2$. The local environment, particular loosely compacted polymer chains around the catalytic sites, limited the access of more bulky substrates. A follow up work from Pomposo *et al.* demonstrated that Cu^{2+} -containing SCNPs catalyzed the water-phase radical polymerization.²³⁸ Cu^{2+} -containing SCNPs as compared to laccase showed much better thermostability. Cu^{2+} -containing SCNPs can catalyzed many other reactions, like alkyne-azide click reaction and epoxidation of C=C bonds. Zimmerman and coworkers showed that Cu^{2+} -containing SCNPs with low toxicity even catalyzed alkyne-azide click reaction within live cells.²³⁹

Other than Cu^{2+} ions, Pt^{2+} ,²⁴² Pd^{2+} ,^{240, 243} Ru^{2+} ,²⁴⁴ Rh^+ ,²⁴⁵ Ir^+ ,²⁴⁶ and Ti^{4+} ²⁴⁷ have been studied in SCNPs as catalysts for various reactions. Knofel *et al.* designed Pt^{2+} -containing polystyrene SCNPs using triphenylphosphine as a ligand.²⁴⁸ With phosphine ligands, it is possible to study the coordination in solution using ³¹P NMR spectroscopy. Interestingly, they found that triphenylphosphine were all bound to Pt^{2+} ions in two different configurations. Pt^{2+} -containing polystyrene SCNPs were as active as monomeric complex $\text{cis-Pt}(\text{PPh}_3)_2\text{Cl}_2$ for amination of allyl alcohol but recyclable and reusable through simple dialysis. Zhang *et al.* synthesized Ti^{4+} -containing SCNPs using chiral salen ligands in water-soluble

PNIPAM.²⁴⁷ Those Ti^{4+} -containing SCNPs were active for asymmetric sulfoxidation reaction with high activity (conversion, 85%~99%) within 1 h and the enantioselectivity reached 95-98%.²⁴⁷ The catalytic efficiency was greatly improved when increasing the hydrophobicity of substrates and retaining high enantioselectivity. Those catalysts were also recyclable up to 8 times by simply using the LCST transition of PNIPAM.²⁴⁹ Lemcoff and coworkers reported the preparation of π -bound metal-containing SCNPs from polyolefins.^{250, 251} Instead of polymerizing complicated ligands, they used ring-opening polymerization to synthesize poly(1,5-cyclooctadiene) with 1,5-diene repeating units. The presence of π bonds could coordinate Rh^+ and Ir^+ through ligand exchange. Using the cross coupling of phenyl boronic acid and 4-nitrobenzaldehyde as an example, Rh^+ -containing SCNPs showed a moderate activity but a unique selectivity to homo-coupling to form biphenyl (>99%). N-heterocyclic carbenes (NHCs) are a strong ligand to a variety of metals through metal-C bonds. NHCs also shows interesting σ donation to transition metals to stabilize metals in the air and promote their reactivity. Lambert *et al.* designed Pd^{2+} -containing SCNPs from a copolymer of water-soluble PEG-grafted PS and 4-vinylbenzylethylbenzimidazolium chloride (Figure 12b). Pd^{2+} bound with benzimidazolium to form Pd^{2+} -NHC coordination resulted in the formation of SCNPs with a hydrodynamic diameter of 9.7 nm. Pd^{2+} -NHC in SCNPs were very active for the Suzuki coupling reaction of 4-iodotoluene and phenyl boronic acid. SCNPs showed a 100% conversion within 5 h while that of the molecular benchmark $\text{Pd}(\text{OAc})_2$ was 24 h.²⁴⁰

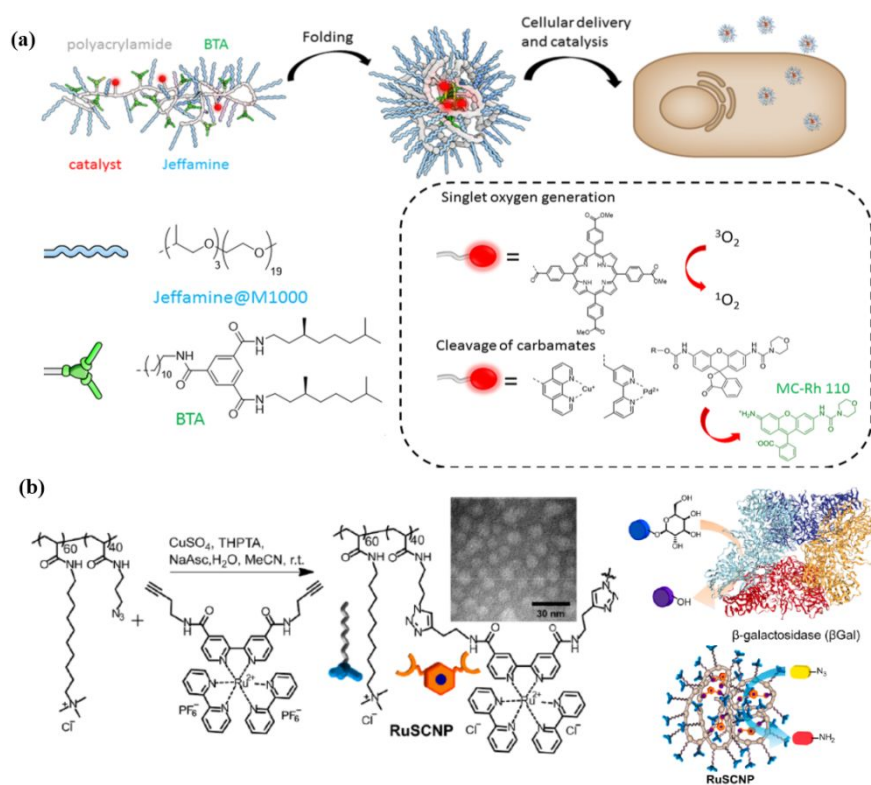


Figure 13. (a) Scheme to illustrate the folding of SCNPs and the catalysis in enzymes and its corresponding chemical structures.²⁶⁶ (b) Chemical structure of Ru^{2+} -containing SCNPs and concept of dual catalysis in enzyme.³¹ Figure (a) reproduced from Ref. 266, copyright 2018 American Chemical Society, Doi: 10.1021/jacs.8b00122;²⁶⁶ Figure (b) reproduced from Ref. 31, copyright 2020 American Chemical Society.³¹

Control of the localized coordination environments of metal sites is the key to improving their reactivity. For examples, natural metalloenzymes have the catalytic metal(s) confined in hydrophobic

pockets around folded proteins. One can mimic such hydrophobic pockets in similar hydrophobic domains in metal-containing SCNPs.^{252, 253} The studies from Meijer and Palmans have extensively

addressed the challenges in control the localized coordination environments of metal sites, including hydrophobic pockets and chiral structures. The benzene-1,3,5-tricarboxamide (BTA) moieties often used for control over the folding structures of SCNPs can stack 1-D helically through three hydrogen bonds.²⁵⁴ Using BTAs in water soluble copolymers, a family of SCNPs with hydrophobic pockets have been designed.²⁵⁵⁻²⁶⁴ The formation of those supramolecular structures through multiple hydrogen bonds was found to be essential for catalysis. For example, in L-proline-containing SCNPs, only SCNPs with the structuring element formed by BTA stacking were active for aldol reactions of *p*-nitrobenzaldehyde and cyclohexanone.²⁶⁵ Those hydrophobic domains possibly isolated L-proline (catalytic sites) from the bulk medium. Together with the improvement of the local concentration of the substrates around active site, the hydrophobic interaction was the key to receive high activity. With triphenylphosphine ligands, Ru²⁺-containing SCNPs prepared in a similar fashion were active for hydrogenation of cyclohexanone and oxidation of secondary alcohols in water (Figure 12c).²⁴¹ The presence of hydrophobic domains had a profound impact on the selectivity. For the oxidation of secondary alcohols, when a cocktail mixture of cyclohexanol, 4-tetrahydropyranol and 4-tert-butylcyclohexanol were examined in acetone, Ru²⁺-containing SCNPs showed nearly identical reactivity for all three alcohols. In contrast, the reactivity of Ru²⁺-containing SCNPs was significantly different when the oxidation was carried out in water. A faster turnover toward the oxidation of 4-tert-butylcyclohexanol was seen among the three substrates. The hydrophobic domains in SCNPs therefore provided proximity to certain substrates that were favorable to access the metal site. With DPA and phenanthroline, Cu²⁺-containing SCNPs were designed for the click reactions of azides and alkynes. There was a dramatic enhancement in reactivity when incorporating Cu²⁺ ions in SCNPs.

One of the advantages to use metal-containing SCNPs is to enhance the stability of metal catalysts in water. As confined within collapsed polymer chains, the biological toxicity of metal ions can be reduced. Although their catalytic efficiency is still too low compared to that of metalloenzymes, it is possible to use metal-containing SCNPs to catalyze reaction in living systems as a "true" synthetic enzyme. Palmans and coworkers used BTA-containing SCNPs to catalyze a catalytic cleavage of protective of rhodamine-based fluorophores (Figure 13a).²⁶⁶ When coordinated with Cu⁺ and Pd²⁺ ions, those SCNPs catalyzed carbamate cleavage reactions for fluorophores both in solution and in cellular media. There was little impact from the HeLa cell to the catalytic carbamate cleavage reactions. More recently, Zimmerman's group designed intracellular catalysis system using Ru²⁺-containing SCNPs (Figure 13b).³¹ Ru²⁺-containing SCNPs could catalyze photochemical reduction of azide-containing fluorogenic rhodamine110 which was fluorescent after reduction. Ru²⁺-containing SCNPs could further bound with another enzyme (2-3 SCNPs per enzyme by *avaergae*), β -galactosidase (β Gal), that catalyzes β -galactosides hydrolysis reaction. The SCNP- β Gal conjugates were able to catalyze a tandem reaction intracellularly. A complex fluorogenic molecule, azido phenyl carbonate β -galactocoumarin, was used for this purpose. Ru²⁺-containing SCNPs first catalyzed the photoreduction of azido and then the cleavage of phenyl carbonate to expose β -galactocoumarin. Subsequently, β -galactocoumarin underwent hydrolysis to turn on the fluorescence of coumarin. 20% of conversion was reached after 10 min within

HeLa cells. Those results are remarkable and potentially bridge the gap between synthetic and natural enzymes in bio-related catalysis.

6. Summary and outlook

We have reviewed the recent advances of metal/polymer hybridization through non-covalent M-L coordination to design multifunctional materials. Coordinating metal ions with synthetic polymers provides a valuable strategy to control the synergetic outcomes such as optical, mechanical and catalytic functionalities of hybrids. On one hand, the built-in non-covalent networks through the dynamic M-L coordination enable the self-healing and recoverable toughness in elastic polymers. The coordination strength enables the precise control of the self-healing efficiency and the recovery proficiency of toughness. On the other hand, synthetic polymers endow the stimuli-responsiveness to metals and provide positive catalytic enhancement to metal sites. With luminescent metals, coupling synthetic polymers with metal enables adaptive behaviors of hybrids, *i.e.*, varying the luminescent emission of hybrids in response to the change of environment. With catalytically active metals, synthetic polymers offer secondary coordination environment to metals that opens up new opportunities to design bioinspired catalysts as synthetic mimics of metalloenzymes.

Although loading metals on synthetic polymers is not new, there are many more functionalities and new synergies through hybridization yet to be discovered. In the light of bioinspired catalysis, metal/polymer hybrids still have plenty of rooms to improve and explore. The current knowledge is only limited to a few model reactions using hybrid catalysts with one type of metal sites. As for enzymatic catalysis, it is common to see the cooperativity among a number of enzymes to convert substrates in a convergent cascade. Previous studies from Finn *et al.* suggested the rolling mechanism in between dendritic catalysts and dendritic substrates.²¹⁹ Rolling instead of diffusing can enhance the reaction kinetics by three magnitudes. It is, therefore, convincing that integrating multiple catalytic sites on synthetic polymers possibly improves the catalytic efficiency of consecutive reactions, if those catalytic sites are encodable in sequence as well. How to encode multiple catalytic metals in polymers, particular facing the challenges of the dynamic coordination, have not been realized yet, although there are some examples in supramolecules.²⁶⁷ Additionally, more sophisticated cooperativity, *e.g.*, with enzymes and nanocatalysts, can be coupled in those hybrid catalysts as demonstrated by Zimmerman *et al.*³¹

There has been rising attention in switchable materials that have multiple mechanical states in response to external stimuli. The M-L coordination has lots of potentials in the design of those switchable materials. As discussed earlier in the Sections 2 and 3, the coordination is stimuli-responsive, *e.g.*, nearly universal response to the pH change in pyridine-containing ligands. In lanthanide complexes, moisture can disrupt the Ln-N coordination. Recent examples also show the response of the M-L coordination to light, as a more robust and spatial/temporal controllable stimulus. In the example reported by Wu *et al.*, the two coordination states of Ru²⁺-thioether and Ru²⁺-H₂O are light-switchable to control the network strength.²⁶⁸ The other example from Johnson *et al.* also suggests that the Pd²⁺ complexes with bis-pyridyl dithienylethene are light-

switchable to control the network topology and the mechanical strength of polymer/metal hybrids.²⁶⁹ The new development of those adaptive M-L bindings can further lead to the design of light-activated actuators and soft robotics. Moreover, all those changes in mechanical states can be coupled with optical properties of metals in form of absorption and luminescence. It will also be possible to use simple optical tools as a readout of mechanical strength of those materials.

Conflicts of interest

There are no conflicts to declare.

Acknowledgements

J.H. is grateful for the continuous financial support from the University of Connecticut, the Green Emulsions, Micelles and Surfactants (GEMS) Center, ACS petroleum research foundation, and the National Science Foundation (CBET-1705566). G.W. is grateful for the financial support of Zhejiang Provincial Natural Science Foundation of China (grant No. LY19E030002) and Ningbo Municipal Science and Technology Bureau (grant No. 2019A610133).

Notes and References

- F. M. Winnik, *Macromolecules*, 1990, **23**, 233-242.
- N. A. Platé, T. L. Lebedeva and L. I. Valuev, *Polym. J.*, 1999, **31**, 21-27.
- X. Zhu, D. Avoco, H. Liu and A. Benrebouh, 2004.
- A. Lendlein and R. S. Trask, *Multifunctional Materials*, 2018, **1**, 010201.
- A. Juris, V. Balzani, F. Barigelli, S. Campagna, P. Belsler and A. von Zelewsky, *Coord. Chem. Rev.*, 1988, **84**, 85-277.
- M. J. MacLachlan, M. Ginzburg, N. Coombs, T. W. Coyle, N. P. Raju, J. E. Greedan, G. A. Ozin and I. Manners, *Science*, 2000, **287**, 1460-1463.
- Y. Sun and Y. Xia, *Analyst*, 2003, **128**, 686-691.
- N. E. Leadbeater and M. Marco, *Chem. Rev.*, 2002, **102**, 3217-3274.
- Y. Li, M. Beijs, S. Laurent, L. v. Elst, R. N. Muller, H. T. Duong, A. B. Lowe, T. P. Davis and C. Boyer, *Macromolecules*, 2012, **45**, 4196-4204.
- H. Yersin and W. J. Finkenzeller, *Highly Efficient OLEDs with Phosphorescent Materials*, 2008, 1-97.
- Z. Nie, D. Fava, E. Kumacheva, S. Zou, G. C. Walker and M. Rubinstein, *Nat. Mater.*, 2007, **6**, 609-614.
- J. He, X. Huang, Y.-C. Li, Y. Liu, T. Babu, M. A. Aronova, S. Wang, Z. Lu, X. Chen and Z. Nie, *J. Am. Chem. Soc.*, 2013, **135**, 7974-7984.
- C. Yi, Y. Yang, B. Liu, J. He and Z. Nie, *Chem. Soc. Rev.*, 2020, **49**, 465-508.
- L. Liu, R. Aleisa, Y. Zhang, J. Feng, Y. Zheng, Y. Yin and W. Wang, *Angew. Chem. Int.*, 2019, **131**, 16453-16459.
- N. Zou, G. Chen, X. Mao, H. Shen, E. Choudhary, X. Zhou and P. Chen, *ACS nano*, 2018, **12**, 5570-5579.
- G. Chen, Y. Wang, M. Yang, J. Xu, S. J. Goh, M. Pan and H. Chen, *J. Am. Chem. Soc.*, 2010, **132**, 3644-3645.
- G. E. Oosterom, J. N. Reek, P. C. Kamer and P. W. van Leeuwen, *Angew. Chem. Int.*, 2001, **40**, 1828-1849.
- K. Liu, N. Zhao and E. Kumacheva, *Chem. Soc. Rev.*, 2011, **40**, 656-671.
- P. Yin, D. Li and T. Liu, *Chem. Soc. Rev.*, 2012, **41**, 7368-7383.
- C. Yi, S. Zhang, K. T. Webb and Z. Nie, *Acc. Chem. Res.*, 2017, **50**, 12-21.
- B. Gao, M. J. Rozin and A. R. Tao, *Nanoscale*, 2013, **5**, 5677-5691.
- P. Chen, Q. Li, S. Grindy and N. Holten-Andersen, *J. Am. Chem. Soc.*, 2015, **137**, 11590-11593.
- G. Weng, S. Thanneeru and J. He, *Adv. Mater.*, 2018, **30**, 1706526.
- X. Zhou, L. Wang, Z. Wei, G. Weng and J. He, *Adv. Funct. Mater.*, 2019, **29**, 1903543.
- Q. Zhu, K. Van Vliet, N. Holten - Andersen and A. Miserez, *Adv. Funct. Mater.*, 2019, **29**, 1808191.
- L. Shi, H. Carstensen, K. Hölzl, M. Lunzer, H. Li, J. Hilborn, A. Ovsianikov and D. A. Ossipov, *Chem. Mater.*, 2017, **29**, 5816-5823.
- N. Holten-Andersen, M. J. Harrington, H. Birkedal, B. P. Lee, P. B. Messersmith, K. Y. C. Lee and J. H. Waite, *PNAS* 2011, **108**, 2651-2655.
- X. Cui, Y. Song, J.-P. Wang, J.-K. Wang, Q. Zhou, T. Qi and G. L. Li, *Polymer*, 2019, **174**, 143-149.
- J. Suriboot, C. E. Hobbs, W. Guzman, H. S. Bazzi and D. E. Bergbreiter, *Macromolecules*, 2015, **48**, 5511-5516.
- Y. Niu, L. K. Yeung and R. M. Crooks, *J. Am. Chem. Soc.*, 2001, **123**, 6840-6846.
- J. Chen, K. Li, J. S. L. Shon and S. C. Zimmerman, *J. Am. Chem. Soc.*, 2020, **142**, 4565-4569.
- W. P. Brezinski, M. Karayilan, K. E. Clary, N. G. Pavlopoulos, S. Li, L. Fu, K. Matyjaszewski, D. H. Evans, R. S. Glass and D. L. Lichtenberger, *Angew. Chem. Int.*, 2018, **57**, 11898-11902.
- C. S. K. Mak and W. K. Chan, *Highly efficient OLEDs with phosphorescent materials*, 2008, 329-362.
- Y. Yan, J. Zhang, L. Ren and C. Tang, *Chem. Soc. Rev.*, 2016, **45**, 5232-5263.
- S. V. Eliseeva and J.-C. G. Bünzli, *Chem. Soc. Rev.*, 2010, **39**, 189-227.
- A. de Bettencourt-Dias, *Luminescence of lanthanide ions in coordination compounds and nanomaterials*, John Wiley & Sons, 2014.
- J. B. Beck and S. J. Rowan, *J. Am. Chem. Soc.*, 2003, **125**, 13922-13923.
- H. S. Jung, P. S. Kwon, J. W. Lee, J. I. Kim, C. S. Hong, J. W. Kim, S. Yan, J. Y. Lee, J. H. Lee and T. Joo, *J. Am. Chem. Soc.*, 2009, **131**, 2008-2012.
- J. Maiti, B. Pokhrel, R. Boruah and S. K. Dolui, *Sens. Actuators B Chem.*, 2009, **141**, 447-451.
- S. C. Yu, X. Gong and W. K. Chan, *Macromolecules*, 1998, **31**, 5639-5646.
- S. C. Yu, S. Hou and W. K. Chan, *Macromolecules*, 1999, **32**, 5251-5256.
- S. C. Yu, S. Hou and W. K. Chan, *Macromolecules*, 2000, **33**, 3259-3273.
- W. Y. Ng, X. Gong and W. K. Chan, *Chem. Mater.*, 1999, **11**, 1165-1170.
- J. R. Kumpfer and S. J. Rowan, *J. Am. Chem. Soc.*, 2011, **133**, 12866-12874.
- Z. Wei, S. Thanneeru, E. Margaret Rodriguez, G. Weng and J. He, *Soft Matter*, 2020, **16**, 2276-2284.
- A. Heller, *J. Am. Chem. Soc.*, 1966, **88**, 2058-2059.
- Y. Haas and G. Stein, *J. Phys. Chem.*, 1971, **75**, 3668-3677.
- J. Chrysochoos, *Spectrosc. Lett.*, 1972, **5**, 57-67.
- S. J. Rowan and J. B. Beck, *Faraday Discuss.*, 2005, **128**, 43-53.
- S.-G. Liu, J.-L. Zuo, Y.-Z. Li and X.-Z. You, *J. Mol. Struct.*, 2004, **705**, 153-157.
- W. Weng, J. B. Beck, A. M. Jamieson and S. J. Rowan, *J. Am. Chem. Soc.*, 2006, **128**, 11663-11672.
- R. Shunmugam and G. N. Tew, *J. Am. Chem. Soc.*, 2005, **127**, 13567-13572.
- Q. Zhang, S. Niu, L. Wang, J. Lopez, S. Chen, Y. Cai, R. Du, Y. Liu, J. C. Lai and L. Liu, *Adv. Mater.*, 2018, **30**, 1801435.
- Z. Wang, C. Xie, C. Yu, G. Fei, Z. Wang and H. Xia, *Macromol. Rapid Commun.*, 2018, **39**, 1700678.
- C. Hu, M. X. Wang, L. Sun, J. H. Yang, M. Zrínyi and Y. M. Chen, *Macromol. Rapid Commun.*, 2017, **38**, 1600788.
- S. Liu, J. Ling, K. Li, F. Yao, O. Oderinde, Z. Zhang and G. Fu, *COMPOS SCI TECHNOL*, 2017, **145**, 62-70.
- Q.-F. Li, S. Chu, E. Li, M. Li, J.-T. Wang and Z. Wang, *Dyes Pigm.*, 2020, **174**, 108091.
- D. W. Balkenende, S. Coulibaly, S. Balog, Y. C. Simon, G. L. Fiore and C. Weder, *J. Am. Chem. Soc.*, 2014, **136**, 10493-10498.
- R. B. Martin and J. A. Lissfelt, *J. Am. Chem. Soc.*, 1956, **78**, 938-940.
- R. Shunmugam and G. N. Tew, *Polym. Adv. Technol.*, 2007, **18**, 940-945.
- R. Shunmugam and G. N. Tew, *Polym. Adv. Technol.*, 2008, **19**, 596-601.
- J. Yuan, X. Fang, L. Zhang, G. Hong, Y. Lin, Q. Zheng, Y. Xu, Y. Ruan, W. Weng and H. Xia, *J. Mater. Chem.*, 2012, **22**, 11515-11522.
- Z. Zhou, Z. Wang, Y. Tang, Y. Zheng and Q. Wang, *J. Mater. Sci.*, 2019, **54**, 2526-2534.
- Q. Zhu, L. Zhang, K. Van Vliet, A. Miserez and N. Holten-Andersen, *ACS Appl. Mater. Interfaces*, 2018, **10**, 10409-10418.
- C. Yang, J. Xu, R. Zhang, Y. Zhang, Z. Li, Y. Li, L. Liang and M. Lu, *Sens. Actuators B Chem.*, 2013, **177**, 437-444.
- A. Balamurugan, M. Reddy and M. Jayakannan, *J. Mater. Chem. A*, 2013, **1**, 2256-2266.
- Y. Yao, Y. Wang, Z. Li and H. Li, *Langmuir*, 2015, **31**, 12736-12741.

68. K. Meng, C. Yao, Q. Ma, Z. Xue, Y. Du, W. Liu and D. Yang, *Adv. Sci.*, 2019, **6**, 1802112.
69. B. Yang, H. Zhang, H. Peng, Y. Xu, B. Wu, W. Weng and L. Li, *Polym. Chem.*, 2014, **5**, 1945-1953.
70. Y. Yamamoto, S. Sawa, Y. Funada, T. Morimoto, M. Falkenström, H. Miyasaka, S. Shishido, T. Ozeki, K. Koike and O. Ishitani, *J. Am. Chem. Soc.*, 2008, **130**, 14659-14674.
71. A. K. Saha, K. Kross, E. D. Kloszewski, D. A. Upson, J. L. Toner, R. A. Snow, C. D. V. Black and V. C. Desai, *J. Am. Chem. Soc.*, 1993, **115**, 11032-11033.
72. M. Yao and W. Chen, *Anal. Chem.*, 2011, **83**, 1879-1882.
73. F. Fueyo-González, E. Garcia-Fernandez, D. Martínez, L. Infantes, A. Orte, J. A. González-Vera and R. Herranz, *ChemComm*, 2020, **56**, 5484-5487.
74. L. Natrajan, J. Pécaut, M. Mazzanti and C. LeBrun, *Inorg. Chem.*, 2005, **44**, 4756-4765.
75. A. M. Nonat, A. J. Harte, K. Sénéchal-David, J. P. Leonard and T. Gunnlaugsson, *Dalton Trans.*, 2009, 4703-4711.
76. E. M. Surrender, S. J. Bradberry, S. A. Bright, C. P. McCoy, D. C. Williams and T. Gunnlaugsson, *J. Am. Chem. Soc.*, 2017, **139**, 381-388.
77. C. P. McCoy, F. Stomeo, S. E. Plush and T. Gunnlaugsson, *Chem. Mater.*, 2006, **18**, 4336-4343.
78. Q.-F. Li, X. Du, L. Jin, M. Hou, Z. Wang and J. Hao, *J. Mater. Chem. C*, 2016, **4**, 3195-3201.
79. S. J. Bradberry, G. Dee, O. Kotova, C. P. McCoy and T. Gunnlaugsson, *ChemComm*, 2019, **55**, 1754-1757.
80. G. Anderegg, F. Arnaud-Neu, R. Delgado, J. Felcman and K. Popov, *Pure Appl. Chem.*, 2005, **77**, 1445-1495.
81. T. Singha Mahapatra, H. Singh, A. Maity, A. Dey, S. K. Pramanik, E. Suresh and A. Das, *J. Mater. Chem. C*, 2018, **6**, 9756-9766.
82. L. Shi, P. Ding, Y. Wang, Y. Zhang, D. Ossipov and J. Hilborn, *Macromol. Rapid Commun.*, 2019, **40**, 1800837.
83. H. Tan, Q. Li, C. Ma, Y. Song, F. Xu, S. Chen and L. Wang, *Biosensors and Bioelectronics*, 2015, **63**, 566-571.
84. H. Chen, Y. Xie, A. M. Kirillov, L. Liu, M. Yu, W. Liu and Y. Tang, *ChemComm*, 2015, **51**, 5036-5039.
85. Y. Song, J. Chen, D. Hu, F. Liu, P. Li, H. Li, S. Chen, H. Tan and L. Wang, *Sens. Actuators B Chem.*, 2015, **221**, 586-592.
86. M. Xu, Z. Gao, Q. Zhou, Y. Lin, M. Lu and D. Tang, *Biosens. Bioelectron.*, 2016, **86**, 978-984.
87. Y. Liu, S. Zhou, L. Fan and H. Fan, *Microchim. Acta*, 2016, **183**, 2605-2613.
88. M. D. Yilmaz and H. A. Oktem, *Anal. Chem.*, 2018, **90**, 4221-4225.
89. Z. Zhou, J. Gu, X. Qiao, H. Wu, H. Fu, L. Wang, H. Li and L. Ma, *Sens. Actuators B Chem.*, 2019, **282**, 437-442.
90. L. Fabbrizzi, M. Licchelli, P. Pallavicini, D. Sacchi and A. Taglietti, *Analyst*, 1996, **121**, 1763-1768.
91. B. Valeur and I. Leray, *Coord. Chem. Rev.*, 2000, **205**, 3-40.
92. L. Prodi, F. Bolletta, M. Montalti and N. Zaccheroni, *Coord. Chem. Rev.*, 2000, **205**, 59-83.
93. Y. Mei, P. A. Bentley and W. Wang, *Tetrahedron Lett.*, 2006, **47**, 2447-2449.
94. H. Yersin, A. F. Rausch, R. Czerwiec, T. Hofbeck and T. Fischer, *Coord. Chem. Rev.*, 2011, **255**, 2622-2652.
95. S. W. Thomas, G. D. Joly and T. M. Swager, *Chem. Rev.*, 2007, **107**, 1339-1386.
96. X.-Y. Chen, X. Yang and B. J. Holliday, *J. Am. Chem. Soc.*, 2008, **130**, 1546-1547.
97. P. T. Furuta, L. Deng, S. Garon, M. E. Thompson and J. M. Fréchet, *J. Am. Chem. Soc.*, 2004, **126**, 15388-15389.
98. M. A. Baldo, D. F. O'Brien, M. E. Thompson and S. R. Forrest, *Phys. Rev. B*, 1999, **60**, 14422-14428.
99. S. Lamansky, P. Djurovich, D. Murphy, F. Abdel-Razzaq, H.-E. Lee, C. Adachi, P. E. Burrows, S. R. Forrest and M. E. Thompson, *J. Am. Chem. Soc.*, 2001, **123**, 4304-4312.
100. M. A. Rawashdeh-Omary, J. M. Lopez-de-Luzuriaga, M. D. Rashdan, O. Elbjairami, M. Monge, M. Rodriguez-Castillo and A. Laguna, *J. Am. Chem. Soc.*, 2009, **131**, 3824-3825.
101. J. Wang, Q. He, C. Wang and W. Bu, *Soft Matter*, 2018, **14**, 31-34.
102. S. Y. An, D. Arunbabu, S. M. Noh, Y. K. Song and J. K. Oh, *ChemComm*, 2015, **51**, 13058-13070.
103. S. Burattini, B. W. Greenland, D. Chappell, H. M. Colquhoun and W. Hayes, *Chem. Soc. Rev.*, 2010, **39**, 1973-1985.
104. Z. Wei, J. H. Yang, J. Zhou, F. Xu, M. Zrínyi, P. H. Dussault, Y. Osada and Y. M. Chen, *Chem. Soc. Rev.*, 2014, **43**, 8114-8131.
105. F. Herbst, D. Döhler, P. Michael and W. H. Binder, *Macromol. Rapid Commun.*, 2013, **34**, 203-220.
106. M. A. Tasdelen, *Polym. Chem.*, 2011, **2**, 2133-2145.
107. G. M. Scheutz, J. J. Lessard, M. B. Sims and B. S. Sumerlin, *J. Am. Chem. Soc.*, 2019, **141**, 16181-16196.
108. Y. Chen and Z. Guan, *ChemComm*, 2014, **50**, 10868-10870.
109. Y. Chen, A. M. Kushner, G. A. Williams and Z. Guan, *Nat. Chem.*, 2012, **4**, 467.
110. S. Burattini, H. M. Colquhoun, J. D. Fox, D. Friedmann, B. W. Greenland, P. J. Harris, W. Hayes, M. E. Mackay and S. J. Rowan, *ChemComm*, 2009, 6717-6719.
111. G. Jiang, C. Liu, X. Liu, G. Zhang, M. Yang, Q. Chen and F. Liu, *J. Macromol. Sci. A*, 2010, **47**, 335-342.
112. D. C. Tuncaboylu, M. Sari, W. Oppermann and O. Okay, *Macromolecules*, 2011, **44**, 4997-5005.
113. D. C. Tuncaboylu, A. Argun, M. Sahin, M. Sari and O. Okay, *Polymer*, 2012, **53**, 5513-5522.
114. Y.-L. Rao, A. Chortos, R. Pfattner, F. Lissel, Y.-C. Chiu, V. Feig, J. Xu, T. Kurosawa, X. Gu and C. Wang, *J. Am. Chem. Soc.*, 2016, **138**, 6020-6027.
115. Y. Shi, M. Wang, C. Ma, Y. Wang, X. Li and G. Yu, *Nano Lett.*, 2015, **15**, 6276-6281.
116. Y.-L. Rao, A. Chortos, R. Pfattner, F. Lissel, Y.-C. Chiu, V. Feig, J. Xu, T. Kurosawa, X. Gu, C. Wang, M. He, J. W. Chung and Z. Bao, *J. Am. Chem. Soc.*, 2016, **138**, 6020-6027.
117. Z. Wei, J. He, T. Liang, H. Oh, J. Athas, Z. Tong, C. Wang and Z. Nie, *Polym. Chem.*, 2013, **4**, 4601-4605.
118. H. Lee, N. F. Scherer and P. B. Messersmith, *PNAS*, 2006, **103**, 12999-13003.
119. Q. Li, D. G. Barrett, P. B. Messersmith and N. Holten-Andersen, *ACS nano*, 2016, **10**, 1317-1324.
120. M. S. Menyo, C. J. Hawker and J. H. Waite, *Soft Matter*, 2013, **9**, 10314-10323.
121. J. K. Hirschberg, L. Brunsveld, A. Ramzi, J. A. Vekemans, R. P. Sijbesma and E. Meijer, *Nature*, 2000, **407**, 167-170.
122. H. E. Bryndza, L. K. Fong, R. A. Paciello, W. Tam and J. E. Bercaw, *J. Am. Chem. Soc.*, 1987, **109**, 1444-1456.
123. A. Avdeef, S. R. Sofen, T. L. Bregante and K. N. Raymond, *J. Am. Chem. Soc.*, 1978, **100**, 5362-5370.
124. M. Zhong, R. Wang, K. Kawamoto, B. D. Olsen and J. A. Johnson, *Science*, 2016, **353**, 1264-1268.
125. S. V. Wegner, F. C. Schenk, S. Witzel, F. Bialas and J. P. Spatz, *Macromolecules*, 2016, **49**, 4229-4235.
126. F. Peng, G. Li, X. Liu, S. Wu and Z. Tong, *J. Am. Chem. Soc.*, 2008, **130**, 16166-16167.
127. W. Sun, S. Li, B. Häupler, J. Liu, S. Jin, W. Steffen, U. S. Schubert, H. J. Butt, X. J. Liang and S. Wu, *Adv. Mater.*, 2017, **29**, 1603702.
128. W. Sun, M. Parowatkin, W. Steffen, H. J. Butt, V. Mailänder and S. Wu, *Adv. Healthc. Mater.*, 2016, **5**, 467-473.
129. X. Xu, Q. Zhang, K. Liu, N. Liu, Y. Han, W. Chen, C. Xie, P. Li and J. He, *Polym. Chem.*, 2019, **10**, 3585-3596.
130. S. W. Taylor, D. B. Chase, M. H. Emptage, M. J. Nelson and J. H. Waite, *Inorg. Chem.*, 1996, **35**, 7572-7577.
131. N. Holten-Andersen, G. E. Fantner, S. Hohlbauch, J. H. Waite and F. W. Zok, *Nat. Mater.*, 2007, **6**, 669-672.
132. F. Peng, G. Li, X. Liu, S. Wu and Z. Tong, *J. Am. Chem. Soc.*, 2008, **130**, 16166-16167.
133. M. J. Harrington, A. Masic, N. Holten-Andersen, J. H. Waite and P. Fratzl, *Science*, 2010, **328**, 216-220.
134. M. Krogsgaard, M. A. Behrens, J. S. Pedersen and H. Birkedal, *Biomacromolecules*, 2013, **14**, 297-301.
135. J. V. Alegre-Requena, M. Häring, R. P. Herrera and D. D. Díaz, *New J. Chem.*, 2016, **40**, 8493-8501.
136. E. Filippidi, T. R. Cristiani, C. D. Eisenbach, J. H. Waite, J. N. Israelachvili, B. K. Ahn and M. T. Valentine, *Science*, 2017, **358**, 502-505.
137. P. M. Lopez-Perez, R. M. P. da Silva, I. Strehin, P. H. J. Kouwer, S. C. G. Leeuwenburgh and P. B. Messersmith, *Macromolecules*, 2017, **50**, 8698-8706.
138. H. Ceylan, M. Urel, T. S. Erkal, A. B. Tekinay, A. Dana and M. O. Guler, *Adv. Funct. Mater.*, 2013, **23**, 2081-2090.

- 139.Z. Li, Y. Shan, X. Wang, H. Li, K. Yang and Y. Cui, *Chem. Eng. J.*, 2020, 124932.
- 140.W. Chen, Y. Bu, D. Li, Y. Liu, G. Chen, X. Wan and N. Li, *J. Mater. Chem. C*, 2020, **8**, 900-908.
- 141.S. W. Taylor, G. W. Luther III and J. H. Waite, *Inorg. Chem.*, 1994, **33**, 5819-5824.
- 142.R. H. Holm, P. Kennepohl and E. I. Solomon, *Chem. Rev.*, 1996, **96**, 2239-2314.
- 143.N. Holten-Andersen, A. Jaishankar, M. J. Harrington, D. E. Fullenkamp, G. DiMarco, L. He, G. H. McKinley, P. B. Messersmith and K. Y. C. Lee, *J. Mater. Chem. B*, 2014, **2**, 2467-2472.
- 144.A. Andersen, M. Krogsgaard and H. Birkedal, *Biomacromolecules*, 2017, **19**, 1402-1409.
- 145.S. Hou and P. X. Ma, *Chem. Mater.*, 2015, **27**, 7627-7635.
- 146.R. M. Roat-Malone, *Bioinorganic chemistry: a short course*, John Wiley & Sons, 2007.
- 147.M. Kierstan and C. Bucke, *Biotechnol. Bioeng.*, 2000, **67**, 726.
- 148.P. Sikorski, F. Mo, G. Skjåk-Bræk and B. T. Stokke, *Biomacromolecules*, 2007, **8**, 2098-2103.
- 149.M. Kierstan and C. Bucke, *Biotechnol. Bioeng.*, 1977, **19**, 387.
- 150.K. Zhang, Q. Feng, J. Xu, X. Xu, F. Tian, K. W. K. Yeung and L. Bian, *Adv. Funct. Mater.*, 2017, **27**, 1701642.
- 151.K. Zhang, W. Yuan, K. Wei, B. Yang, X. Chen, Z. Li, Z. Zhang and L. Bian, *Small*, 2019, **15**, 1900242.
- 152.L. Shi, F. Wang, W. Zhu, Z. Xu, S. Fuchs, J. Hilborn, L. Zhu, Q. Ma, Y. Wang, X. Weng and D. A. Ossipov, *Adv. Funct. Mater.*, 2017, **27**, 1700591.
- 153.Q. Zhang, S. Niu, L. Wang, J. Lopez, S. Chen, Y. Cai, R. Du, Y. Liu, J.-C. Lai, L. Liu, C.-H. Li, X. Yan, C. Liu, J. B.-H. Tok, X. Jia and Z. Bao, *Adv. Mater.*, 2018, **30**, 1801435.
- 154.Y.-L. Rao, V. Feig, X. Gu, G.-J. Nathan Wang and Z. Bao, *J POLYM SCI POLY CHEM*, 2017, **55**, 3110-3116.
- 155.D. Mozhdzhi, J. A. Neal, S. C. Grindy, Y. Cordeau, S. Ayala, N. Holten-Andersen and Z. Guan, *Macromolecules*, 2016, **49**, 6310-6321.
- 156.S. Bonnet, B. Limburg, J. D. Meeldijk, R. J. Klein Gebbink and J. A. Killian, *J. Am. Chem. Soc.*, 2011, **133**, 252-261.
- 157.C. Xie, W. Sun, H. Lu, A. Kretzschmann, J. Liu, M. Wagner, H.-J. Butt, X. Deng and S. Wu, *Nat. Commun.*, 2018, **9**, 3842.
- 158.J. Liu, C. Xie, A. Kretzschmann, K. Koynov, H.-J. Butt and S. Wu, *Adv. Mater.*, 2020, **32**, 1908324.
- 159.D. Yu, X. Zhao, C. Zhou, C. Zhang and S. Zhao, *Macromol. Chem. Phys.*, 2017, **218**, 1600519.
- 160.E. S. Epstein, L. Martinetti, R. H. Kollarigowda, O. Carey-De La Torre, J. S. Moore, R. H. Ewoldt and P. V. Braun, *J. Am. Chem. Soc.*, 2019, **141**, 3597-3604.
- 161.L. Zhang, Z. Liu, X. Wu, Q. Guan, S. Chen, L. Sun, Y. Guo, S. Wang, J. Song and E. M. Jeffries, *Adv. Mater.*, 2019, **31**, 1901402.
- 162.S. Götz, R. Geitner, M. Abend, M. Siegmann, S. Zechel, J. Vitz, S. Gräfe, M. Schmitt, J. Popp and M. D. Hager, *Macromol. Rapid Commun.*, 2018, **39**, 1800495.
- 163.J.-C. Lai, X.-Y. Jia, D.-P. Wang, Y.-B. Deng, P. Zheng, C.-H. Li, J.-L. Zuo and Z. Bao, *Nat. Commun.*, 2019, **10**, 1-9.
- 164.J.-C. Lai, L. Li, D.-P. Wang, M.-H. Zhang, S.-R. Mo, X. Wang, K.-Y. Zeng, C.-H. Li, Q. Jiang and X.-Z. You, *Nat. Commun.*, 2018, **9**, 1-9.
- 165.C.-H. Li, C. Wang, C. Keplinger, J.-L. Zuo, L. Jin, Y. Sun, P. Zheng, Y. Cao, F. Lissel, C. Linder, X.-Z. You and Z. Bao, *Nat. Chem.*, 2016, **8**, 618-624.
- 166.X.-Y. Jia, J.-F. Mei, J.-C. Lai, C.-H. Li and X.-Z. You, *Macromol. Rapid Commun.*, 2016, **37**, 952-956.
- 167.B. Sandmann, B. Happ, S. Kupfer, F. H. Schacher, M. D. Hager and U. S. Schubert, *Macromol. Rapid Commun.*, 2015, **36**, 604-609.
- 168.S. Bode, R. K. Bose, S. Matthes, M. Ehrhardt, A. Seifert, F. H. Schacher, R. M. Paulus, S. Stumpf, B. Sandmann, J. Vitz, A. Winter, S. Hoepfner, S. J. Garcia, S. Spange, S. van der Zwaag, M. D. Hager and U. S. Schubert, *Polym. Chem.*, 2013, **4**, 4966-4973.
- 169.M. Enke, L. Köps, S. Zechel, J. C. Brendel, J. Vitz, M. D. Hager and U. S. Schubert, *Macromol. Rapid Commun.*, 2018, **39**, 1700742.
- 170.J. Pignaneli, Z. Qian, X. Gu, M. J. Ahamed and S. Rondeau-Gagné, *New J. Chem.*, 2020, **44**, 8977-8985.
- 171.M. Enke, F. Jehle, S. Bode, J. Vitz, M. J. Harrington, M. D. Hager and U. S. Schubert, *Macromol. Chem. Phys.*, 2017, **218**, 1600458.
- 172.M. Chen, W. Wang, H. Chen, L. Bai, Z. Xue, D. Wei, H. Yang and Y. Niu, *Macromol. Res.*, 2019, **27**, 96-104.
- 173.D. Mozhdzhi, S. Ayala, O. R. Cromwell and Z. Guan, *J. Am. Chem. Soc.*, 2014, **136**, 16128-16131.
- 174.Y. Kobayashi, T. Hirase, Y. Takashima, A. Harada and H. Yamaguchi, *Polym. Chem.*, 2019, **10**, 4519-4523.
- 175.J. P. Gong, Y. Katsuyama, T. Kurokawa and Y. Osada, *Adv. Mater.*, 2003, **15**, 1155-1158.
- 176.J. P. Gong, *Soft Matter*, 2010, **6**, 2583-2590.
- 177.T. Nakajima, H. Sato, Y. Zhao, S. Kawahara, T. Kurokawa, K. Sugahara and J. P. Gong, *Adv. Funct. Mater.*, 2012, **22**, 4426-4432.
- 178.T. Nakajima, H. Furukawa, Y. Tanaka, T. Kurokawa, Y. Osada and J. P. Gong, *Macromolecules*, 2009, **42**, 2184-2189.
- 179.E. Ducrot, Y. Chen, M. Bulters, R. P. Sijbesma and C. Creton, *Science*, 2014, **344**, 186-189.
- 180.E. Ducrot and C. Creton, *Adv. Funct. Mater.*, 2016, **26**, 2482-2492.
- 181.T. Matsuda, T. Nakajima and J. P. Gong, *Chem. Mater.*, 2019, **31**, 3766-3776.
- 182.J.-Y. Sun, X. Zhao, W. R. K. Illeperuma, O. Chaudhuri, K. H. Oh, D. J. Mooney, J. J. Vlassak and Z. Suo, *Nature*, 2012, **489**, 133-136.
- 183.C. Hu, M. X. Wang, L. Sun, J. H. Yang, M. Zrínyi and Y. M. Chen, *Macromol. Rapid Commun.*, 2017, **38**, 1600788.
- 184.X. He, C. Zhang, M. Wang, Y. Zhang, L. Liu and W. Yang, *ACS Appl. Mater. Interfaces*, 2017, **9**, 11134-11143.
- 185.S. Hong, D. Sycks, H. F. Chan, S. Lin, G. P. Lopez, F. Guilak, K. W. Leong and X. Zhao, *Adv. Mater.*, 2015, **27**, 4035-4040.
- 186.M. X. Wang, C. H. Yang, Z. Q. Liu, J. Zhou, F. Xu, Z. Suo, J. H. Yang and Y. M. Chen, *Macromol. Rapid Commun.*, 2015, **36**, 465-471.
- 187.X.-H. Wang, F. Song, J. Xue, D. Qian, X.-L. Wang and Y.-Z. Wang, *Polymer*, 2018, **153**, 637-642.
- 188.X. Li, H. Wang, D. Li, S. Long, G. Zhang and Z. Wu, *ACS Appl. Mater. Interfaces*, 2018, **10**, 31198-31207.
- 189.G. Weng, Y. Huang, S. Thanneeru, H. Li, A. Alamri and J. He, *Soft Matter*, 2017, **13**, 5028-5037.
- 190.X. Zhao, *Soft Matter*, 2014, **10**, 672-687.
- 191.X.-H. Wang, F. Song, D. Qian, Y.-D. He, W.-C. Nie, X.-L. Wang and Y.-Z. Wang, *Chem. Eng. J.*, 2018, **349**, 588-594.
- 192.M. S. Menyo, C. J. Hawker and J. H. Waite, *ACS Macro Lett.*, 2015, **4**, 1200-1204.
- 193.C. Ma, Y. Wang, Z. Jiang, Z. Cao, H. Yu, G. Huang, Q. Wu, F. Ling, Z. Zhuang, H. Wang, J. Zheng and J. Wu, *Chem. Eng. J.*, 2020, **399**, 125697.
- 194.M. A. Gonzalez, J. R. Simon, A. Ghoorchian, Z. Scholl, S. Lin, M. Rubinstein, P. Marszalek, A. Chilkoti, G. P. López and X. Zhao, *Adv. Mater.*, 2017, **29**, 1604743.
- 195.Q. Chen, X. Yan, L. Zhu, H. Chen, B. Jiang, D. Wei, L. Huang, J. Yang, B. Liu and J. Zheng, *Chem. Mater.*, 2016, **28**, 5710-5720.
- 196.L. Zhang, Z. Liu, X. Wu, Q. Guan, S. Chen, L. Sun, Y. Guo, S. Wang, J. Song, E. M. Jeffries, C. He, F.-L. Qing, X. Bao and Z. You, *Adv. Mater.*, 2019, **31**, 1901402.
- 197.M. Yan, L. Cao, C. Xu and Y. Chen, *Macromolecules*, 2019, **52**, 4329-4340.
- 198.M. H. Ghanian, H. Mirzadeh and H. Baharvand, *Biomacromolecules*, 2018, **19**, 1646-1662.
- 199.G. Hong, H. Zhang, Y. Lin, Y. Chen, Y. Xu, W. Weng and H. Xia, *Macromolecules*, 2013, **46**, 8649-8656.
- 200.Y. Chen, Z. Tang, Y. Liu, S. Wu and B. Guo, *Macromolecules*, 2019, **52**, 3805-3812.
- 201.Z. Tang, J. Huang, B. Guo, L. Zhang and F. Liu, *Macromolecules*, 2016, **49**, 1781-1789.
- 202.J. Huang, Z. Tang, Z. Yang and B. Guo, *Macromol. Rapid Commun.*, 2016, **37**, 1040-1045.
- 203.J. Liu, Z. Tang, J. Huang, B. Guo and G. Huang, *Polymer*, 2016, **97**, 580-588.
- 204.M. Benaglia, A. Puglisi and F. Cozzi, *Chem. Rev.*, 2003, **103**, 3401-3430.
- 205.D. E. Bergbreiter, J. Tian and C. Hongfa, *Chem. Rev.*, 2009, **109**, 530-582.
- 206.D. E. Bergbreiter, *ACS Macro Lett.*, 2014, **3**, 260-265.
- 207.N. Madhavan, C. W. Jones and M. Weck, *Acc. Chem. Res.*, 2008, **41**, 1153-1165.
- 208.P. Bhyrappa, J. K. Young, J. S. Moore and K. S. Suslick, *J. Am. Chem. Soc.*, 1996, **118**, 5708-5711.
- 209.A. Ellis and L. J. Twyman, *Macromolecules*, 2013, **46**, 7055-7074.
- 210.M. Zhao and R. M. Crooks, *Angew. Chem. Int.*, 1999, **38**, 364-366.

- 211.H. A. Zayas, A. Lu, D. Valade, F. Amir, Z. Jia, R. K. O'Reilly and M. J. Monteiro, *ACS Macro Lett.*, 2013, **2**, 327-331.
- 212.S. Wu, J. Dzubiella, J. Kaiser, M. Drechsler, X. Guo, M. Ballauff and Y. Lu, *Angew. Chem. Int.*, 2012, **51**, 2229-2233.
- 213.Y. Chen, Z. Wang, Y. W. Harn, S. Pan, Z. Li, S. Lin, J. Peng, G. Zhang and Z. Lin, *Angew. Chem. Int.*, 2019, **58**, 11910-11917.
- 214.D. E. Bergbreiter, V. M. Mariagnanam and L. Zhang, *Adv. Mater.*, 1995, **7**, 69-71.
- 215.W. Kramer and C. McCrory, *Chem. Sci.*, 2016, **7**, 2506-2515.
- 216.S. Thanneeru, J. K. Nganga, A. S. Amin, B. Liu, L. Jin, A. M. Angeles-Boza and J. He, *ChemCatChem*, 2017, **9**, 1157-1162.
- 217.W. P. Brezinski, M. Karayilan, K. E. Clary, K. C. McCleary-Petersen, L. Fu, K. Matyjaszewski, D. H. Evans, D. L. Lichtenberger, R. S. Glass and J. Pyun, *ACS Macro Lett.*, 2018, **7**, 1383-1387.
- 218.S. Thanneeru, N. Milazzo, A. Lopes, Z. Wei, A. M. Angeles-Boza and J. He, *J. Am. Chem. Soc.*, 2019, **141**, 4252-4256.
- 219.C. S. McKay and M. G. Finn, *Angew. Chem. Int.*, 2016, **55**, 12643-12649.
- 220.J. A. Trindell, J. Clausmeyer and R. M. Crooks, *J. Am. Chem. Soc.*, 2017, **139**, 16161-16167.
- 221.L. Zhang, Z. Wei, S. Thanneeru, M. Meng, M. Kruzyk, G. Ung, B. Liu and J. He, *Angew. Chem. Int.*, 2019, **131**, 15981-15987.
- 222.G. E. Oosterom, J. N. H. Reek, P. C. J. Kamer and P. W. N. M. van Leeuwen, *Angew. Chem. Int.*, 2001, **40**, 1828-1849.
- 223.J. W. J. Knapen, A. W. van der Made, J. C. de Wilde, P. W. N. M. van Leeuwen, P. Wijkens, D. M. Grove and G. van Koten, *Nature*, 1994, **372**, 659-663.
- 224.A. Ouali, R. Laurent, A.-M. Caminade, J.-P. Majoral and M. Taillefer, *J. Am. Chem. Soc.*, 2006, **128**, 15990-15991.
- 225.C. S. McKay and M. Finn, *Angew. Chem. Int.*, 2016, **128**, 12833-12839.
- 226.T. Yamamoto, T. Yamada, Y. Nagata and M. Sugimoto, *J. Am. Chem. Soc.*, 2010, **132**, 7899-7901.
- 227.J. P. Leonard, M. Fabrizio and S. Paolo, *Curr. Org. Chem.*, 2009, **13**, 1050-1064.
- 228.W. P. Brezinski, M. Karayilan, K. E. Clary, N. G. Pavlopoulos, S. Li, L. Fu, K. Matyjaszewski, D. H. Evans, R. S. Glass, D. L. Lichtenberger and J. Pyun, *Angew. Chem. Int.*, 2018, **57**, 11898-11902.
- 229.Y. Liu and C. C. McCrory, *Nat. Commun.*, 2019, **10**, 1-10.
- 230.F. Wang, W. J. Liang, J. X. Jian, C. B. Li, B. Chen, C. H. Tung and L. Z. Wu, *Angew. Chem. Int.*, 2013, **125**, 8292-8296.
- 231.T. Yu, Y. Zeng, J. Chen, Y. Y. Li, G. Yang and Y. Li, *Angew. Chem. Int.*, 2013, **52**, 5631-5635.
- 232.E. Verde-Sesto, A. Arbe, A. Moreno, D. Cangialosi, Á. Alegría, J. Colmenero and J. A. Pomposo, *Mater. Horiz.*, 2020.
- 233.J. Rubio-Cervilla, E. González and J. A. Pomposo, *Nanomaterials*, 2017, **7**, 341.
- 234.O. Altintas and C. Barner - Kowollik, *Macromol. Rapid Commun.*, 2012, **33**, 958-971.
- 235.A. Latorre - Sánchez and J. A. Pomposo, *Polym. Int.*, 2016, **65**, 855-860.
- 236.H. Rothfuss, N. D. Knöfel, P. W. Roesky and C. Barner-Kowollik, *J. Am. Chem. Soc.*, 2018, **140**, 5875-5881.
- 237.A. Sanchez-Sanchez, A. Arbe, J. Colmenero and J. A. Pomposo, *ACS Macro Lett.*, 2014, **3**, 439-443.
- 238.A. Sanchez-Sanchez, A. Arbe, J. Kohlbrecher, J. Colmenero and J. A. Pomposo, *Macromol. Rapid Commun.*, 2015, **36**, 1592-1597.
- 239.Y. Bai, X. Feng, H. Xing, Y. Xu, B. K. Kim, N. Baig, T. Zhou, A. A. Gewirth, Y. Lu, E. Oldfield and S. C. Zimmerman, *J. Am. Chem. Soc.*, 2016, **138**, 11077-11080.
- 240.R. Lambert, A.-L. Wirocius, S. Garmendia, P. Berto, J. Vignolle and D. Taton, *Polym. Chem.*, 2018, **9**, 3199-3204.
- 241.M. Artar, E. R. J. Souren, T. Terashima, E. W. Meijer and A. R. A. Palmans, *ACS Macro Lett.*, 2015, **4**, 1099-1103.
- 242.N. D. Knöfel, H. Rothfuss, J. Willenbacher, C. Barner - Kowollik and P. W. Roesky, *Angew. Chem. Int.*, 2017, **56**, 4950-4954.
- 243.J. Willenbacher, O. Altintas, V. Trouillet, N. Knöfel, M. J. Monteiro, P. W. Roesky and C. Barner-Kowollik, *Polym. Chem.*, 2015, **6**, 4358-4365.
- 244.M. Artar, T. Terashima, M. Sawamoto, E. Meijer and A. R. Palmans, *J. POLYM SCI POL CHEM*, 2014, **52**, 12-20.
- 245.A. Levy, R. Feinstein and C. E. Diesendruck, *J. Am. Chem. Soc.*, 2019, **141**, 7256-7260.
- 246.S. Mavila, I. Rozenberg and N. G. Lemcoff, *Chem. Sci.*, 2014, **5**, 4196-4203.
- 247.Y. Zhang, R. Tan, M. Gao, P. Hao and D. Yin, *Green Chem.*, 2017, **19**, 1182-1193.
- 248.N. D. Knöfel, H. Rothfuss, J. Willenbacher, C. Barner-Kowollik and P. W. Roesky, *Angew. Chem. Int.*, 2017, **56**, 4950-4954.
- 249.Y. Zhang, W. Wang, W. Fu, M. Zhang, Z. Tang, R. Tan and D. Yin, *ChemComm*, 2018, **54**, 9430-9433.
- 250.S. Mavila, I. Rozenberg and N. G. Lemcoff, *Chem. Sci.*, 2014, **5**, 4196-4203.
- 251.S. Mavila, C. E. Diesendruck, S. Linde, L. Amir, R. Shikler and N. G. Lemcoff, *Angew. Chem. Int.*, 2013, **125**, 5879-5882.
- 252.T. Terashima, A. Nomura, M. Ito, M. Ouchi and M. Sawamoto, *Angew. Chem. Int.*, 2011, **50**, 7892-7895.
- 253.T. Terashima, M. Ouchi, T. Ando and M. Sawamoto, *Polym. J.*, 2011, **43**, 770-777.
- 254.C. Kulkarni, E. Meijer and A. R. Palmans, *Acc. Chem. Res.*, 2017, **50**, 1928-1936.
- 255.T. Terashima, T. Mes, T. F. A. De Greef, M. A. J. Gillissen, P. Besenius, A. R. A. Palmans and E. W. Meijer, *J. Am. Chem. Soc.*, 2011, **133**, 4742-4745.
- 256.T. Mes, R. van der Weegen, A. R. A. Palmans and E. W. Meijer, *Angew. Chem. Int.*, 2011, **50**, 5085-5089.
- 257.N. Hosono, A. R. A. Palmans and E. W. Meijer, *ChemComm*, 2014, **50**, 7990-7993.
- 258.M. A. J. Gillissen, I. K. Voets, E. W. Meijer and A. R. A. Palmans, *Polym. Chem.*, 2012, **3**, 3166-3174.
- 259.N. Hosono, A. M. Kushner, J. Chung, A. R. A. Palmans, Z. Guan and E. W. Meijer, *J. Am. Chem. Soc.*, 2015, **137**, 6880-6888.
- 260.P. J. M. Stals, C.-Y. Cheng, L. van Beek, A. C. Wauters, A. R. A. Palmans, S. Han and E. W. Meijer, *Chem. Sci.*, 2016, **7**, 2011-2015.
- 261.P. J. M. Stals, M. A. J. Gillissen, T. F. E. Paffen, T. F. A. de Greef, P. Lindner, E. W. Meijer, A. R. A. Palmans and I. K. Voets, *Macromolecules*, 2014, **47**, 2947-2954.
- 262.G. M. ter Huurne, M. A. J. Gillissen, A. R. A. Palmans, I. K. Voets and E. W. Meijer, *Macromolecules*, 2015, **48**, 3949-3956.
- 263.E. Huerta, B. van Genabeek, P. J. M. Stals, E. W. Meijer and A. R. A. Palmans, *Macromol. Rapid Commun.*, 2014, **35**, 1320-1325.
- 264.M. A. J. Gillissen, T. Terashima, E. W. Meijer, A. R. A. Palmans and I. K. Voets, *Macromolecules*, 2013, **46**, 4120-4125.
- 265.E. Huerta, P. J. Stals, E. Meijer and A. R. Palmans, *Angew. Chem. Int.*, 2013, **125**, 2978-2982.
- 266.Y. Liu, S. Pujals, P. J. Stals, T. Paulöhr, S. I. Presolski, E. Meijer, L. Albertazzi and A. R. Palmans, *J. Am. Chem. Soc.*, 2018, **140**, 3423-3433.
- 267.L. Wang, B. Song, Y. Li, L. Gong, X. Jiang, M. Wang, S. Lu, X.-Q. Hao, Z. Xia, Y. Zhang, S. W. Hla and X. Li, *J. Am. Chem. Soc.*, 2020, **142**, 9809-9817.
- 268.J. Liu, C. Xie, A. Kretzschmann, K. Koynov, H. J. Butt and S. Wu, *Adv. Mater.*, 2020, **32**, 1908324.
- 269.Y. Gu, E. A. Alt, H. Wang, X. Li, A. P. Willard and J. A. Johnson, *Nature*, 2018, **560**, 65-69.

ARTICLE

Table of Contents

